Meson vacuum phenomenology in a three-flavor linear sigma model with (axial-)vector mesons

D. Parganlija,[1,2,*] P. Kovács,[2,3,†] Gy. Wolf,[3,‡] F. Giacosa,[2,§] and D. H. Rischke[2,4,‖]

[1]*Institute for Theoretical Physics, Vienna University of Technology, Wiedner Hauptstrasse 8-10, A-1040 Vienna, Austria*
[2]*Institute for Theoretical Physics, Johann Wolfgang Goethe University, Max-von-Laue-Strasse 1, D-60438 Frankfurt am Main, Germany*
[3]*Institute for Particle and Nuclear Physics, Wigner Research Center for Physics, Hungarian Academy of Sciences, H-1525 Budapest, Hungary*
[4]*Frankfurt Institute for Advanced Studies, Ruth-Moufang-Strasse 1, D-60438 Frankfurt am Main, Germany*

(Received 7 August 2012; published 8 January 2013)

We study scalar, pseudoscalar, vector, and axial-vector mesons with nonstrange and strange quantum numbers in the framework of a linear sigma model with global chiral $U(N_f)_L \times U(N_f)_R$ symmetry. We perform a global fit of meson masses, decay widths, as well as decay amplitudes. The quality of the fit is, for a hadronic model that does not consider isospin-breaking effects, surprisingly good. We also investigate the question whether the scalar $\bar{q}q$ states lie below or above 1 GeV and find the scalar states above 1 GeV to be preferred as $\bar{q}q$ states. Additionally, we also describe the axial-vector resonances as $\bar{q}q$ states.

DOI: 10.1103/PhysRevD.87.014011 PACS numbers: 12.39.Fe, 12.40.Yx, 14.40.Be, 14.40.Df

I. INTRODUCTION

Understanding the meson mass spectrum in the region below 2 GeV is one of the fundamental problems of QCD. While the quark model seems to work very well for many resonances (see, for instance, the summary in Ref. [1]), some fundamental questions, such as the constituent quark content of scalar and axial-vector resonances, are still unanswered.

The quark content of the scalar mesons has been a matter of debate for many decades [2]. The Particle Data Group (PDG) [1] suggests the existence of five $I(J^{PC}) = 0(0^{++})$ states in the region below 1.8 GeV: $f_0(500)$, $f_0(980)$, $f_0(1370)$, $f_0(1500)$, and $f_0(1710)$. Also the existence of a sixth state, $f_0(1790)$, close to, but distinct from, $f_0(1710)$ has been claimed [3]. Additionally, there are scalar resonances in the isotriplet and in the isodoublet sector as well: the $I = 1$ states $a_0(980)$ and $a_0(1450)$ are well established; the existence of the $I = 1/2$ state $K_0^\star(800)$ (or κ) is confirmed by some [4] and disputed by other authors [5], whereas the $I = 1/2$ scalar kaon, $K_0^\star(1430)$, is an established resonance.

A description of all mentioned scalar states as $\bar{q}q$ states is not possible for a simple reason: the number of physical resonances is much larger than the number of resonances that can be constructed within a $\bar{q}q$ picture of mesons. Explicitly, there is only one $I(J^{PC}) = 0(0^{++})$ state that can be constructed from the (nonstrange) u and d quarks (provided they are degenerate). Denoting this state as σ_N we obtain $\sigma_N \equiv (\bar{u}u + \bar{d}d)/\sqrt{2}$. An additional $I(J^{PC}) = 0(0^{++})$ state can be constructed, if the strange quark is considered as well: the pure strange state $\sigma_S \equiv \bar{s}s$. Since σ_N and σ_S have the same $I(J^{PC})$ quantum numbers, we expect the physical spectrum to consist of mixed, rather than pure, states of σ_N and σ_S; however, such mixing will, of course, produce exactly two new states. These states will correspond to at most two of the mentioned five (six) f_0 states, and the natural question is then: *which two*?

Similarly, in both the $I = 1$ and $I = 1/2$ sectors one can construct only one quark-antiquark resonance. Restricting for example to electric charge $+1$, one has the states $a_0^+ = \bar{d}u$ and $K_0^{*+} = \bar{s}u$. The state $a_0^+ = \bar{d}u$ can be assigned to $a_0(980)$ or $a_0(1450)$, and $K_0^{*+} = \bar{s}u$ to $K_0^\star(800)$ or $K_0^\star(1430)$. The question is: *which is the correct assignment?*

An answer to these questions is inevitably complicated for several reasons. First, as already indicated, states with the same $I(J^{PC})$ quantum numbers are expected to mix—this needs to be considered in particular in the scalar sector due to the large number of physical resonances. Second, basic features (pole mass and decay width) of some scalar mesons [e.g., $f_0(500)$] are notoriously difficult to determine experimentally, which makes it nontrivial to determine the structure of these states [see, e.g., Ref. [6] for an example regarding the $f_0(500)$ resonance and Ref. [7] for an example regarding $f_0(1370)$].

The question of how to correctly determine the quark structure of the mesons is not only restricted to the scalar sector. More recently, also the nature of the axial-vector mesons, most notably $a_1(1260)$, but also that of the isoscalar states $f_1(1285)$, $f_1(1525)$, and the kaonic state $K_1(1270)$ [or $K_1(1400)$, see the discussion in Ref. [8] and references therein] have been investigated. Should one interpret the isotriplet resonance $a_1(1260)$ as a quark-antiquark state, as the quark model suggests (e.g. $a_1^+ = \bar{d}u$), or is this state a broad $\rho\pi$ molecular state?

Understanding these issues is not only crucial for hadron vacuum spectroscopy but is also important at nonzero temperatures and densities, because the correct identification of the chiral partner of the pion and of the ρ meson is necessary for a proper description of the in-medium

*denisp@hep.itp.tuwien.ac.at
†kovacs.peter@wigner.mta.hu
‡wolf.gyorgy@wigner.mta.hu
§giacosa@th.physik.uni-frankfurt.de
‖drischke@th.physik.uni-frankfurt.de

properties of hadrons [9]. In fact, if the $a_1(1260)$ is (predominantly) a quark-antiquark state, it is the chiral partner of the ρ meson, with which it becomes degenerate at large T and μ [10]. The chiral partner of the pion is the scalar-isoscalar state $\sigma_N \equiv (\bar{u}u + \bar{d}d)/\sqrt{2}$ which has been identified with the lightest scalar state $f_0(500)$ in many works. However, as various theoretical results for the vacuum have shown, and as we shall present in detail in this work, this assignment is not correct: it turns out that $f_0(1370)$ emerges as the chiral partner of the pion.

Last but not least, the question of the origin of hadron masses is important. One aims to understand to which extent the quark condensate, $\langle \bar{q}q \rangle$, and the gluon condensate, $\langle G^{\mu\nu}G_{\mu\nu} \rangle$, generate the hadron masses. To give an example, which condensate is predominantly responsible for the mass of the ρ meson? And related to this, how will the mass of the ρ (and that of other resonances) change in the medium?

The answers to all these fundamental questions are in principle contained in the QCD Lagrangian. Unfortunately, QCD cannot be solved by analytic means from first principles in the low-energy domain. For this reason, effective theories have been developed which share some of the underlying symmetries of QCD. The QCD Lagrangian exhibits, in addition to the local $SU(3)_c$ color symmetry and the discrete C, P, and T symmetries, a global chiral $U(N_f)_L \times U(N_f)_R \equiv U(1)_V \times U(1)_A \times SU(N_f)_V \times SU(N_f)_A$ symmetry which is broken in several ways: spontaneously (due to the chiral condensate $\langle \bar{q}q \rangle = \langle \bar{q}_R q_L + \bar{q}_L q_R \rangle \neq 0$ [11]), explicitly (due to nonvanishing quark masses), as well as at the quantum level [the $U(1)_A$ anomaly [12]].

In the framework of effective theories the chiral symmetry of QCD can be realized along two lines: linearly [13] and nonlinearly [14]. In the former case one obtains the so-called linear sigma model: both scalar and pseudoscalar degrees of freedom are present and vectors as well as axial vectors can be included into the model in a straightforward manner [15–19]. Note that an important advantage of linear sigma models is the possibility to investigate the state of matter at large values of temperature and chemical potential (e.g., in the region of the chiral transition, i.e., where chiral symmetry is restored [20,21]). Every linear sigma model contains so-called chiral partners—states that mix with each other under axial transformations—that become degenerate when chiral symmetry is restored. In the nonlinear realization (i.e., the nonlinear sigma models), the scalar and the (axial-)vector states are integrated out and the pseudoscalar states are the only degrees of the freedom: one obtains the Lagrangian of chiral perturbation theory [22]. If the vector mesons are not integrated out, one is left with chiral perturbation theory with vector mesons (see, e.g., Ref. [23] and references therein).

In this paper, we present a linear sigma model containing scalar, pseudoscalar, vector, and axial-vector mesons with both nonstrange and strange quantum numbers. Although this project represents a straightforward implementation of the principles of the linear realization of chiral symmetry as already outlined in Ref. [17], this is—to our knowledge—the first time that all these degrees of freedom are considered within a single linear chiral framework. In view of the large number of the fields involved, our model shall be referred to as the "extended linear sigma model." Moreover, we also exploit a "classical" symmetry of the QCD Lagrangian in the chiral limit: the dilatation symmetry. This symmetry is broken by quantum effects (trace anomaly) and generates, through dimensional transmutation, the QCD low-energy scale Λ_{QCD}. We describe this phenomenon by including a dilaton field in our model. The associated potential for the dilaton field encodes the trace anomaly by an explicit breaking of dilatation symmetry. We assume that, except for terms associated with the $U(1)_A$ anomaly and nonzero quark masses, all other interactions are dilatation invariant. Assuming in addition analyticity in the fields (i.e., absence of divergences in the Lagrangian in the limit of vanishing fields), the number of terms appearing in the Lagrangian is finite. The fluctuations of the dilaton field correspond to the glueball degree of freedom. In this work, we neglect the coupling of the glueball with the other mesonic degrees of freedom. Formally, this can be justified by taking the large-N_c limit. In a future work, we also plan to study the coupling of the glueball to mesons in our framework, similar to the $N_f = 2$ study of Ref. [24].

In Refs. [15,25], we have already presented a linear sigma model with vector and axial-vector mesons for two flavors. Comparing our model with experimental data for meson vacuum phenomenology led us to conclude that the scalar $\bar{q}q$ states are located in the energy region above 1 GeV in the hadron mass spectrum. Explicitly, we concluded that the resonances $f_0(1370)$ and $a_0(1450)$ are strongly favored to be scalar quarkonia. The present work is more general: we now consider three flavors both in the (pseudo)scalar and (axial-)vector channels in order to ascertain whether the conclusion of Ref. [15] is still valid once strange mesons are considered. We emphasize that, as discussed in Ref. [15], all fields entering our model describe pure quark-antiquark states. The reason is that masses and decay widths of our theoretical states scale as N_c^0 and N_c^{-1}, respectively, where N_c is the number of colors; thus all decay widths vanish in the large-N_c limit. Note that the inclusion of strange mesons provides us with a large amount of very precise data (in general, decisively more precise than in the case of nonstrange mesons [1]). As a consequence, our model parameters are much more constrained than in Ref. [15]. Preliminary results of this work have already been presented in Ref. [26].

In order to (i) test the performance of a linear sigma model in describing the overall phenomenology of (pseudo)scalar and (axial-)vector mesons and (ii) ascertain which scalar states are predominantly quarkonia, we perform a global fit in which 21 experimentally known quantities (decay constants, masses, and decay widths as well as amplitudes) are included. The situation in the scalar-isoscalar sector is

extremely uncertain because five (six) resonances, $f_0(500)$, $f_0(980)$, $f_0(1370)$, $f_0(1500)$, and $f_0(1710)$ [and, possibly in the future, $f_0(1790)$] are listed in the PDG. In addition, the $f_0(500)$ and $f_0(1370)$ decay widths and branching ratios are poorly known and $f_0(980)$ suffers from a distortion by the $K\bar{K}$ threshold. Moreover, a scalar glueball state with a bare mass of about 1.5–1.7 GeV as predicted by lattice QCD [27] can sizably affect the masses and the branching ratios of the scalar states above 1 GeV, that is, $f_0(1370)$, $f_0(1500)$, and $f_0(1710)$ [28]. In view of all these reasons, we do *not* include the scalar-isoscalar states into the fit. We note that, although the coupling of the glueball state to the other mesons is not considered in this paper, it does not affect our global fit. We do, however, include the isotriplet and isodoublet quark-antiquark scalar states and we test all four combinations $a_0(1450)/K_0^\star(1430)$, $a_0(980)/K_0^\star(800)$, $a_0(980)/K_0^\star(1430)$, and $a_0(1450)/K_0^\star(800)$. Quite remarkably, the outcome of the fit is univocal: only the pair $a_0(1450)/K_0^\star(1430)$ yields a good fit, while the other combinations do not. We thus conclude that the $I = 1$ and $I = 1/2$ quark-antiquark scalar resonances lie above 1 GeV. In fact, the quality of our fit is surprisingly good. We describe *all* experimental quantities with an average error of 5%, and most of them even to much better precision. We perceive this to be a remarkable achievement within an (in principle, quite simple) effective model for the strong interaction.

We then study the two scalar-isoscalar quark-antiquark states in our model: a consequence of our fit is their mass in the large-N_c limit. These masses turn out to be about 1.36 GeV and 1.53 GeV, respectively. Varying large-N_c suppressed parameters which cannot be determined by our fit, one can also study their decays: the nonstrange quark-antiquark state is well described by $f_0(1370)$ and the heavier $\bar{s}s$ state might be $f_0(1710)$. Turning to the axial-vector channel, both masses and decays are well described by assuming the axial-vector resonances $a_1(1260)$, $f_1(1285)$, $f_1(1525)$, and $K_1(1270)$ as (predominantly) quark-antiquark states. Detailed calculations of all formulas used in this paper as well as further discussion are presented in Ref. [29].

The outline of the paper is as follows. In Sec. II we discuss the $U(3)_L \times U(3)_R$ linear sigma model with vector and axial-vector mesons. In Sec. III we discuss the global fit and its consequences and in Sec. IV we present our conclusions. We defer detailed calculations to Appendixes A and B. Our units are $\hbar = c = 1$; the metric tensor is $g_{\mu\nu} = \mathrm{diag}(+, -, -, -)$.

II. THE MODEL

A. Lagrangian

In this section we present our model: a linear sigma model with (axial-)vector mesons and global chiral $U(3)_L \times U(3)_R$ symmetry. To this end, we discuss some important criteria for the construction of its Lagrangian.

The aim of our work is to emulate the properties of the QCD Lagrangian in our effective approach. This implies the necessity to consider as many symmetries of QCD as possible. The QCD Lagrangian possesses various symmetries: local (gauge) invariance with respect to the color group $SU(3)_c$, discrete C, P, and T symmetries, global chiral symmetry $U(3)_L \times U(3)_R$ (which is exact in the chiral limit), and also the classical dilatation (scale) symmetry. The local color symmetry is automatically fulfilled when working with colorless hadronic degrees of freedom. The discrete and chiral symmetries impose severe constraints on the terms which are kept in the Lagrangian; still, infinitely many are allowed. Indeed, in some older versions of the linear sigma model, terms with dimension larger than four were considered; see for example Refs. [17,18,30]. In these approaches chiral symmetry was promoted to a *local symmetry*, up to the vector-meson mass term which breaks this symmetry explicitly. Sigma models with local chiral symmetry require the inclusion of terms of order larger than four in the fields in order to correctly describe experimental data. This procedure obviously breaks renormalizability, but this is not an issue because a hadronic theory is obviously not fundamental and is supposed to be valid only up to a mass scale of 1–2 GeV. Still, the problem of constraining the number of terms affects these effective approaches of QCD.

We then turn our attention to the last of the mentioned symmetries of QCD: the dilatation symmetry. It plays a key role to justify why we retain only a *finite* number of terms [31]. Let us recall some of the basic features of the dilatation symmetry in the pure gauge sector of QCD: The Yang-Mills (YM) Lagrangian (QCD without quarks) is classically invariant under dilatations, but this symmetry is broken at the quantum level. The divergence of the corresponding current is the trace of the energy-momentum tensor $T^{\mu\nu}_{\mathrm{YM}}$ of the YM Lagrangian $(T_{\mathrm{YM}})^\mu_\mu = \frac{\beta(g)}{4g} G^a_{\mu\nu} G^{a,\mu\nu} \neq 0$, where $G^a_{\mu\nu}$ is the gluon field-strength tensor and $\beta(g)$ the beta function of YM theory. At the composite level, one can parametrize this situation by introducing the dilaton field G, which is described by the Lagrangian [32]

$$\mathcal{L}_{\mathrm{dil}} = \frac{1}{2}(\partial_\mu G)^2 - \frac{1}{4}\frac{m_G^2}{\Lambda^2}\left(G^4 \ln\frac{G^2}{\Lambda^2} - \frac{G^4}{4}\right). \qquad (1)$$

The dilatation symmetry is explicitly broken by the scale Λ under the logarithm. The minimum of the dilaton potential is realized for $G_0 = \Lambda$; upon shifting $G \to G_0 + G$, a particle with mass m_G emerges, which is interpreted as the scalar glueball. The numerical value has been evaluated in lattice QCD and reads $m_G \sim 1.6$ GeV [27]. In the large-N_c limit, $m_G \sim N_c^0$, while the n-glueball vertex $\sim N_c^{2-n}$ [33]. Applying this to Eq. (1), we observe that $\Lambda \sim N_c$. In the large-N_c limit, the glueball self-interaction terms vanish and the glueball becomes a free field.

We are now ready to present our Lagrangian. It follows from requiring symmetry under C, P, T, (global) chiral [15,19,29], as well as dilatation transformations. In accordance with QCD, we take the latter two symmetries to be

explicitly broken only by nonzero quark masses, and dilatation symmetry to be explicitly broken only by the dilaton potential in Eq. (1) as well as the $U_A(1)$ anomaly. Therefore, all other terms in the Lagrangian must be dilatation invariant and thus carry mass dimension equal to four. This would in principle still allow for an infinite number of terms. However, assuming in addition that there are no terms with nonanalytic powers of the field variables makes the number of possible terms finite.

Explicitly, the Lagrangian of the model has the form

$$\begin{aligned}\mathcal{L} &= \mathcal{L}_{\mathrm{dil}} + \mathrm{Tr}[(D_\mu\Phi)^\dagger(D_\mu\Phi)] - m_0^2\left(\frac{G}{G_0}\right)^2\mathrm{Tr}(\Phi^\dagger\Phi) - \lambda_1[\mathrm{Tr}(\Phi^\dagger\Phi)]^2 - \lambda_2\mathrm{Tr}(\Phi^\dagger\Phi)^2 - \frac{1}{4}\mathrm{Tr}(L_{\mu\nu}^2 + R_{\mu\nu}^2)\\ &+ \mathrm{Tr}\left[\left(\left(\frac{G}{G_0}\right)^2\frac{m_1^2}{2} + \Delta\right)(L_\mu^2 + R_\mu^2)\right] + \mathrm{Tr}[H(\Phi + \Phi^\dagger)] + c_1(\det\Phi - \det\Phi^\dagger)^2 + i\frac{g_2}{2}(\mathrm{Tr}\{L_{\mu\nu}[L^\mu, L^\nu]\}\\ &+ \mathrm{Tr}\{R_{\mu\nu}[R^\mu, R^\nu]\}) + \frac{h_1}{2}\mathrm{Tr}(\Phi^\dagger\Phi)\mathrm{Tr}(L_\mu^2 + R_\mu^2) + h_2\mathrm{Tr}[|L_\mu\Phi|^2 + |\Phi R_\mu|^2] + 2h_3\mathrm{Tr}(L_\mu\Phi R^\mu\Phi^\dagger)\\ &+ g_3[\mathrm{Tr}(L_\mu L_\nu L^\mu L^\nu) + \mathrm{Tr}(R_\mu R_\nu R^\mu R^\nu)] + g_4[\mathrm{Tr}(L_\mu L^\mu L_\nu L^\nu) + \mathrm{Tr}(R_\mu R^\mu R_\nu R^\nu)]\\ &+ g_5\mathrm{Tr}(L_\mu L^\mu)\mathrm{Tr}(R_\nu R^\nu) + g_6[\mathrm{Tr}(L_\mu L^\mu)\mathrm{Tr}(L_\nu L^\nu) + \mathrm{Tr}(R_\mu R^\mu)\mathrm{Tr}(R_\nu R^\nu)], \end{aligned} \tag{2}$$

where $\mathcal{L}_{\mathrm{dil}}$ is the dilaton term (1) and

$$D^\mu\Phi \equiv \partial^\mu\Phi - ig_1(L^\mu\Phi - \Phi R^\mu) - ieA^\mu[T_3, \Phi], \qquad L^{\mu\nu} \equiv \partial^\mu L^\nu - ieA^\mu[T_3, L^\nu] - \{\partial^\nu L^\mu - ieA^\nu[T_3, L^\mu]\},$$
$$R^{\mu\nu} \equiv \partial^\mu R^\nu - ieA^\mu[T_3, R^\nu] - \{\partial^\nu R^\mu - ieA^\nu[T_3, R^\mu]\}.$$

The quantities Φ, R^μ, and L^μ represent the scalar and vector nonets:

$$\Phi = \sum_{i=0}^{8}(S_i + iP_i)T_i = \frac{1}{\sqrt{2}}\begin{pmatrix}\frac{(\sigma_N + a_0^0) + i(\eta_N + \pi^0)}{\sqrt{2}} & a_0^+ + i\pi^+ & K_0^{\star+} + iK^+\\ a_0^- + i\pi^- & \frac{(\sigma_N - a_0^0) + i(\eta_N - \pi^0)}{\sqrt{2}} & K_0^{\star0} + iK^0\\ K_0^{\star-} + iK^- & \bar{K}_0^{\star0} + i\bar{K}^0 & \sigma_S + i\eta_S\end{pmatrix}, \tag{3}$$

$$L^\mu = \sum_{i=0}^{8}(V_i^\mu + A_i^\mu)T_i = \frac{1}{\sqrt{2}}\begin{pmatrix}\frac{\omega_N + \rho^0}{\sqrt{2}} + \frac{f_{1N} + a_1^0}{\sqrt{2}} & \rho^+ + a_1^+ & K^{\star+} + K_1^+\\ \rho^- + a_1^- & \frac{\omega_N - \rho^0}{\sqrt{2}} + \frac{f_{1N} - a_1^0}{\sqrt{2}} & K^{\star0} + K_1^0\\ K^{\star-} + K_1^- & \bar{K}^{\star0} + \bar{K}_1^0 & \omega_S + f_{1S}\end{pmatrix}^\mu, \tag{4}$$

$$R^\mu = \sum_{i=0}^{8}(V_i^\mu - A_i^\mu)T_i = \frac{1}{\sqrt{2}}\begin{pmatrix}\frac{\omega_N + \rho^0}{\sqrt{2}} - \frac{f_{1N} + a_1^0}{\sqrt{2}} & \rho^+ - a_1^+ & K^{\star+} - K_1^+\\ \rho^- - a_1^- & \frac{\omega_N - \rho^0}{\sqrt{2}} - \frac{f_{1N} - a_1^0}{\sqrt{2}} & K^{\star0} - K_1^0\\ K^{\star-} - K_1^- & \bar{K}^{\star0} - \bar{K}_1^0 & \omega_S - f_{1S}\end{pmatrix}^\mu, \tag{5}$$

where the assignment to physical particles is shown as well.[1] Here, $T_i (i = 0, \ldots, 8)$ denote the generators of $U(3)$, while S_i represents the scalar, P_i the pseudoscalar, V_i^μ the vector, A_i^μ the axial-vector-meson fields, and A^μ is the electromagnetic field. It should be noted that here and below we use the so-called nonstrange-strange basis in the (0–8) sector, defined as

$$\varphi_N = \frac{1}{\sqrt{3}}(\sqrt{2}\varphi_0 + \varphi_8), \qquad \varphi_S = \frac{1}{\sqrt{3}}(\varphi_0 - \sqrt{2}\varphi_8),$$
$$\varphi \in (S_i, P_i, V_i^\mu, A_i^\mu), \tag{6}$$

which is more suitable for our calculations. Moreover, H and Δ are constant external fields defined as

$$H = H_0T_0 + H_8T_8 = \begin{pmatrix}\frac{h_{0N}}{2} & 0 & 0\\ 0 & \frac{h_{0N}}{2} & 0\\ 0 & 0 & \frac{h_{0S}}{\sqrt{2}}\end{pmatrix}, \tag{7}$$

$$\Delta = \Delta_0T_0 + \Delta_8T_8 = \begin{pmatrix}\frac{\tilde{\delta}_N}{2} & 0 & 0\\ 0 & \frac{\tilde{\delta}_N}{2} & 0\\ 0 & 0 & \frac{\tilde{\delta}_S}{\sqrt{2}}\end{pmatrix} \equiv \begin{pmatrix}\delta_N & 0 & 0\\ 0 & \delta_N & 0\\ 0 & 0 & \delta_S\end{pmatrix}. \tag{8}$$

These terms describe the effect of nonzero quark masses in the (pseudo)scalar and (axial-)vector sectors, respectively:

[1]With the exception of the (0–8) sector where particle mixing takes place (see below).

$h_N \sim m_u$, $h_S \sim m_s$, $\delta_N \sim m_u^2$, $\delta_S \sim m_s^2$. Throughout this work we assume exact isospin symmetry for u and d quarks, such that the first two diagonal elements in Eq. (7) and (8) are identical. Thus, only the scalar-isoscalar fields σ_N, σ_S and G, carrying the same quantum numbers as the vacuum, can have nonzero vacuum expectation values (vev's).[2]

In the Lagrangian (2) the following terms break the original $U(3)_L \times U(3)_R [= U(3)_V \times U(3)_A]$ symmetry: (i) the terms proportional to the matrix H and Δ of Eqs. (7) and (8), which describe the explicit symmetry breaking due to the nonzero values of the quark masses in the (pseudo)scalar and (axial-)vector sectors and break $U(3)_A$ if H_0, $\Delta_0 \neq 0$ and $U(3)_V \to SU(2)_V \times U(1)_V$ if H_8, $\Delta_8 \neq 0$ (for more details see, e.g., Ref. [20]), and (ii) the term proportional to the determinant and parametrized by c_1, which breaks the $U(1)_A$ symmetry and describes the axial anomaly, responsible for large mass of the η' meson.

These terms also explicitly break dilatation symmetry because they involve dimensionful coupling constants. This is expected: the first two terms describe the bare quark masses which generate an explicit breaking of dilatation symmetry at the level of the QCD Lagrangian, and the determinant term describes an anomalous breaking of the dilatation symmetry arising from the YM sector of the theory.

The interaction of the meson fields with the dilaton field G enters only in two terms. Upon condensation of the dilaton field, these terms correspond to meson mass terms. In addition, there are interaction terms proportional to one or two powers of the glueball field. Since $G_0 \sim \Lambda \sim N_c$, an $(m+g)$-point vertex involving m-meson lines and g-glueball lines scales as $\sim N_c^{-(m/2+g-1)}$, while an m-point vertex involving m-meson lines scales as $N_c^{1-m/2}$. Thus, vertices with n external lines involving glueballs vanish faster than the corresponding n-point vertices involving only mesons. As a first approximation, we assume that the glueball field completely decouples, so that we neglect it in the following. Effects from coupling the glueball to the other meson fields will be studied in a subsequent work.

Let us now discuss in detail the assignment of fields in Eqs. (3)–(5) If we consider isospin multiplets as single degrees of freedom, then there are 16 resonances that can be described by the model: σ_N, σ_S, $\vec{a}_0$, $K_0^\star$ (scalar); η_N, η_S, $\vec{\pi}$, K (pseudoscalar); ω_N^μ, ω_S^μ, $\vec{\rho}^\mu$, $K^{\star\mu}$ (vector), and f_{1N}^μ, f_{1S}^μ, $\vec{a}_1^\mu$, K_1 (axial vector). All fields in our model represent $\bar{q}q$ states, as discussed in Ref. [15]. If we assign a state from our model to a physical resonance we, therefore, implicitly assume that this resonance is a $\bar{q}q$ state. This assumption can be tested for a multitude of physical resonances in the scalar and axial-vector sectors, as discussed below (in the pseudoscalar and the vector channels, there are no ambiguities).

In the nonstrange sector, we assign the fields $\vec{\pi}$ and η_N to the pion and the nonstrange part of the η and η' mesons, $\eta_N \equiv (\bar{u}u + \bar{d}d)/\sqrt{2}$. The fields ω_N^μ and $\vec{\rho}^\mu$ represent the $\omega(782)$ and $\rho(770)$ vector mesons, respectively, and the fields f_{1N}^μ and $\vec{a}_1^\mu$ represent the $f_1(1285)$ and $a_1(1260)$ mesons, respectively. In the strange sector, we assign the K fields to the kaons; the η_S field is the strange contribution to the physical η and η' fields ($\eta_S \equiv \bar{s}s$); the ω_S, f_{1S}, $K^\star$, and K_1 fields correspond to the $\phi(1020)$, $f_1(1420)$, $K^\star(892)$, and $K_1(1270)$ [or $K_1(1400)$] mesons, respectively.

Unfortunately, the assignment of the scalar fields is substantially less clear. Experimental data suggest existence of five (six) scalar-isoscalar states below 1.8 GeV: $f_0(500)$, $f_0(980)$, $f_0(1370)$, $f_0(1500)$, and $f_0(1710)$ [as well as $f_0(1790)$]. Note that the existence of these five states is acknowledged by the Particle Data Group [1]. [The sixth state, $f_0(1790)$, will not be of importance for the rest of our work because its predominant $\pi\pi$ decay renders it a putative radial excitation of $f_0(1370)$, and our model describes ground-state quarkonia only.]

Our model contains a pure nonstrange isoscalar σ_N and a pure strange isoscalar σ_S. We will demonstrate below that our model yields mixing of σ_N and σ_S, producing a predominantly nonstrange state labeled as f_0^L, and a predominantly strange state labeled as f_0^H. Assignment of the mixed states to physical resonances is ambiguous because, as already discussed, there are five physical states all of which could, in principle, be candidates for f_0^L and f_0^H.

Similarly, the isospin triplet a_0 can be assigned to different physical resonances—although, in this case, there are only two candidate states: $a_0(980)$ and $a_0(1450)$. A preliminary examination of the assignment of the a_0 field has been performed in Ref. [15] where it was concluded that it most likely corresponds to the $a_0(1450)$ resonance [or, equivalently, $a_0(1450)$ rather than $a_0(980)$ was favored to represent a $\bar{q}q$ state]. The discussion in Ref. [15] was limited to nonstrange mesons. In this work, besides the assignment of a_0, we also have to consider possible assignments for the strange scalar field $K_0^\star$; there are also two possibilities: either $K_0^\star(800)$ or $K_0^\star(1430)$.

B. Tree-level masses and mixing terms

After spontaneous symmetry breaking, the fields with nonzero vev's are shifted by their expectation values, namely, $\sigma_{N/S} \to \sigma_{N/S} + \phi_{N/S}$, where we have introduced $\phi_{N/S} \equiv \langle \sigma_{N/S} \rangle$. After substituting the shifted fields into the Lagrangian (2), one obtains the tree-level masses by selecting all terms quadratic in the fields,

[2]In case of isospin breaking, also σ_3 could have a nonzero vev.

$$\mathcal{L}^{\text{quad}} = -\frac{1}{2}S_i[\delta_{ij}\Box + (m_S^2)_{ij}]S_j - \frac{1}{2}P_i[\delta_{ij}\Box + (m_P^2)_{ij}]P_j - \frac{1}{2}V_{i\mu}[(-g^{\mu\nu}\Box + \partial^\mu\partial^\nu)\delta_{ij} - g^{\mu\nu}(m_V^2)_{ij}]V_{j\nu}$$
$$-\frac{1}{2}A_{i\mu}[(-g^{\mu\nu}\Box + \partial^\mu\partial^\nu)\delta_{ij} - g^{\mu\nu}(m_A^2)_{ij}]A_{j\nu} - \frac{1}{2}V_{i\mu}(ig_1 f_{ijk}\phi_k\partial^\mu)S_j - \frac{1}{2}S_i(ig_1 f_{ijk}\phi_k\partial^\nu)V_{j\nu}$$
$$+\frac{1}{2}A_{i\mu}(g_1 d_{ijk}\phi_k\partial^\mu)P_j - \frac{1}{2}P_i(g_1 d_{ijk}\phi_k\partial^\nu)A_{j\nu}, \tag{9}$$

where $(m_S^2)_{ij}$, $(m_P^2)_{ij}$, $(m_V^2)_{ij}$, and $(m_A^2)_{ij}$ are the scalar, pseudoscalar, vector, and axial-vector (squared) mass matrices, respectively (see their explicit expressions in Appendix A). Moreover, f_{ijk} and d_{ijk} are the antisymmetric and symmetric structure constants of $U(3)$. The (squared) mass matrices are in general nondiagonal due to the mixing among particles sitting in the center of a given nonet, and they can be diagonalized by appropriate orthogonal transformations (for details see Appendix A). Besides the mixing inside the nonets there are other mixing terms, namely the last four terms of Eq. (9), which mix different nonets.

In order to eliminate the latter, one performs the following shifts of the (axial-)vector fields:

$$\begin{aligned} f_{1N/S}^\mu &\to f_{1N/S}^\mu + Z_{\eta_{N/S}} w_{f_{1N/S}} \partial^\mu \eta_{N/S}, \\ a_1^{\mu\pm,0} &\to a_1^{\mu\pm,0} + Z_\pi w_{a_1} \partial^\mu \pi^{\pm,0}, \\ K_1^{\mu\pm,0,\bar{0}} &\to K_1^{\mu\pm,0,\bar{0}} + Z_K w_{K_1} \partial^\mu K^{\pm,0,\bar{0}}, \\ K^{\star\mu\pm,0,\bar{0}} &\to K^{\star\mu\pm,0,\bar{0}} + Z_{K^\star} w_{K^\star} \partial^\mu K_0^{\star\pm,0,\bar{0}}. \end{aligned} \tag{10}$$

These shifts produce additional kinetic terms for the pseudoscalar fields. In order to retain the canonical normalization for the latter, one has to introduce wave function renormalization constants,

$$\begin{aligned} &\pi^{\pm,0} \to Z_\pi \pi^{\pm,0}, \qquad K^{\pm,0,\bar{0}} \to Z_K K^{\pm,0,\bar{0}}, \\ &\eta_{N/S} \to Z_{\eta_N/\eta_S}\eta_{N/S}, \qquad K^{\star\mu\pm,0,\bar{0}} \to Z_{K^\star} K^{\star\mu\pm,0,\bar{0}}. \end{aligned} \tag{11}$$

For the sake of simplicity we have grouped together the isotriplet states with the notation $\pi^{\pm,0}$, $a_1^{\mu\pm,0}$ and the isodoublet states with the notation $K^{\pm,0,\bar{0}}$, $K^{\star\mu\pm,0,\bar{0}}$, where $\bar{0}$ refers to $\bar{K}^0$. The coefficients w_i and Z_i are determined in order to eliminate the last four mixing terms in Eq. (9) and to obtain the canonical normalization of the π, η_N, η_S, K, and $K_0^\star$ fields. After some straightforward calculation one finds the explicit expressions:

$$w_{f_{1N}} = w_{a_1} = \frac{g_1\phi_N}{m_{a_1}^2}, \qquad w_{f_{1S}} = \frac{\sqrt{2}g_1\phi_S}{m_{f_{1S}}^2},$$
$$w_{K^\star} = \frac{ig_1(\phi_N - \sqrt{2}\phi_S)}{2m_{K^\star}^2}, \qquad w_{K_1} = \frac{g_1(\phi_N + \sqrt{2}\phi_S)}{2m_{K_1}^2}, \tag{12}$$

$$Z_\pi = Z_{\eta_N} = \frac{m_{a_1}}{\sqrt{m_{a_1}^2 - g_1^2\phi_N^2}},$$
$$Z_K = \frac{2m_{K_1}}{\sqrt{4m_{K_1}^2 - g_1^2(\phi_N + \sqrt{2}\phi_S)^2}}, \tag{13}$$

$$Z_{\eta_S} = \frac{m_{f_{1S}}}{\sqrt{m_{f_{1S}}^2 - 2g_1^2\phi_S^2}},$$
$$Z_{K^\star} = \frac{2m_{K^\star}}{\sqrt{4m_{K^\star}^2 - g_1^2(\phi_N - \sqrt{2}\phi_S)^2}}. \tag{14}$$

It can be seen from the expressions of the wave function renormalization constants that they are always larger than one. Finally, using the explicit expressions found in Appendix A the tree-level (squared) masses for the different nonets are obtained as follows:

$$m_\pi^2 = Z_\pi^2\left[m_0^2 + \left(\lambda_1 + \frac{\lambda_2}{2}\right)\phi_N^2 + \lambda_1\phi_S^2\right] \equiv \frac{Z_\pi^2 h_{0N}}{\phi_N}, \tag{15}$$

$$m_K^2 = Z_K^2\left[m_0^2 + \left(\lambda_1 + \frac{\lambda_2}{2}\right)\phi_N^2 - \frac{\lambda_2}{\sqrt{2}}\phi_N\phi_S + (\lambda_1 + \lambda_2)\phi_S^2\right], \tag{16}$$

$$m_{\eta_N}^2 = Z_\pi^2\left[m_0^2 + \left(\lambda_1 + \frac{\lambda_2}{2}\right)\phi_N^2 + \lambda_1\phi_S^2 + c_1\phi_N^2\phi_S^2\right] \equiv Z_\pi^2\left(\frac{h_{0N}}{\phi_N} + c_1\phi_N^2\phi_S^2\right), \tag{17}$$

$$m_{\eta_S}^2 = Z_{\eta_S}^2\left[m_0^2 + \lambda_1\phi_N^2 + (\lambda_1 + \lambda_2)\phi_S^2 + \frac{c_1}{4}\phi_N^4\right] \equiv Z_{\eta_S}^2\left(\frac{h_{0S}}{\phi_S} + \frac{c_1}{4}\phi_N^4\right), \tag{18}$$

$$m_{\eta_{NS}}^2 = Z_\pi Z_{\pi_S}\frac{c_1}{2}\phi_N^3\phi_S \tag{19}$$

are the (squared) pseudoscalar masses, while

$$m_{a_0}^2 = m_0^2 + \left(\lambda_1 + \frac{3}{2}\lambda_2\right)\phi_N^2 + \lambda_1\phi_S^2, \tag{20}$$

$$m^2_{K_0^\star} = Z^2_{K_0^\star}\Big[m_0^2 + \Big(\lambda_1 + \frac{\lambda_2}{2}\Big)\phi_N^2 + \frac{\lambda_2}{\sqrt{2}}\phi_N\phi_S + (\lambda_1+\lambda_2)\phi_S^2\Big], \tag{21}$$

$$m^2_{\sigma_N} = m_0^2 + 3\Big(\lambda_1 + \frac{\lambda_2}{2}\Big)\phi_N^2 + \lambda_1\phi_S^2, \tag{22}$$

$$m^2_{\sigma_S} = m_0^2 + \lambda_1\phi_N^2 + 3(\lambda_1+\lambda_2)\phi_S^2, \tag{23}$$

$$m^2_{\sigma_{NS}} = 2\lambda_1\phi_N\phi_S \tag{24}$$

are the (squared) scalar masses. The quantities $m^2_{\pi_{NS}}$ and $m^2_{\sigma_{NS}}$ are mixing terms in the nonstrange-strange sector. These mixings can be removed by orthogonal transformations, and the resulting mass eigenstates are found to be

$$m^2_{f_0^H/f_0^L} = \frac{1}{2}\Big[m^2_{\sigma_N} + m^2_{\sigma_S} \pm \sqrt{(m^2_{\sigma_N} - m^2_{\sigma_S})^2 + 4m^4_{\sigma_{NS}}}\Big], \tag{25}$$

$$m^2_{\eta'/\eta} = \frac{1}{2}\Big[m^2_{\eta_N} + m^2_{\eta_S} \pm \sqrt{(m^2_{\eta_N} - m^2_{\eta_S})^2 + 4m^4_{\eta_{NS}}}\Big]. \tag{26}$$

Moreover, the (squared) vector masses are given by

$$m_\rho^2 = m_1^2 + \frac{1}{2}(h_1+h_2+h_3)\phi_N^2 + \frac{h_1}{2}\phi_S^2 + 2\delta_N, \tag{27}$$

$$m^2_{K^\star} = m_1^2 + \frac{1}{4}(g_1^2 + 2h_1 + h_2)\phi_N^2 + \frac{1}{\sqrt{2}}\phi_N\phi_S(h_3 - g_1^2) + \frac{1}{2}(g_1^2 + h_1 + h_2)\phi_S^2 + \delta_N + \delta_S, \tag{28}$$

$$m^2_{\omega_N} = m_\rho^2, \tag{29}$$

$$m^2_{\omega_S} = m_1^2 + \frac{h_1}{2}\phi_N^2 + \Big(\frac{h_1}{2} + h_2 + h_3\Big)\phi_S^2 + 2\delta_S, \tag{30}$$

while the (squared) axial-vector-meson masses are

$$m^2_{a_1} = m_1^2 + \frac{1}{2}(2g_1^2 + h_1 + h_2 - h_3)\phi_N^2 + \frac{h_1}{2}\phi_S^2 + 2\delta_N, \tag{31}$$

$$m^2_{K_1} = m_1^2 + \frac{1}{4}(g_1^2 + 2h_1 + h_2)\phi_N^2 - \frac{1}{\sqrt{2}}\phi_N\phi_S(h_3 - g_1^2) + \frac{1}{2}(g_1^2 + h_1 + h_2)\phi_S^2 + \delta_N + \delta_S, \tag{32}$$

$$m^2_{f_{1N}} = m^2_{a_1}, \tag{33}$$

$$m^2_{f_{1S}} = m_1^2 + \frac{h_1}{2}\phi_N^2 + \Big(2g_1^2 + \frac{h_1}{2} + h_2 - h_3\Big)\phi_S^2 + 2\delta_S. \tag{34}$$

It is interesting to note that in case of vectors and axial vectors there are no mixings in the nonstrange-strange sector.

C. Parameters

The Lagrangian (2) contains 18 parameters (as mentioned above, we neglect the coupling of the glueball with the other mesons in the present work):

$$m_0^2,\ m_1^2,\ c_1,\ \delta_N,\ \delta_S,\ g_1,\ g_2,\ g_3,\ g_4,\ g_5,\ g_6,\ h_{0N},\ h_{0S},\ h_1,\ h_2,\ h_3,\ \lambda_1,\ \lambda_2. \tag{35}$$

We make the following observations regarding the model parameters:

(i) The parameters h_{0N} and h_{0S} model the explicit breaking of the chiral symmetry (ESB) in the (pseudo)scalar sector via the term $\mathrm{Tr}[H(\Phi + \Phi^\dagger)]$; they are uniquely determined from the mass terms of the pion, Eq. (15), and of η_S, the strange part of the η meson [see Eq. (18)], implying that the masses of $\vec{\pi}$ and η_S are generated by ESB.

(ii) The parameters δ_N and δ_S model the explicit symmetry breaking in the vector and axial-vector channels. The ESB arises from nonvanishing quark masses and therefore we employ the correspondence $\delta_N \propto m^2_{u,d}$ and $\delta_S \propto m_s^2$. However, in the vector-meson mass term $\mathrm{Tr}[(m_1^2/2 + \Delta)(L_\mu^2 + R_\mu^2)]$ only the linear combinations $m_1^2/2 + \delta_{N/S}$ appear. Therefore, it is possible to redefine $m_1^2/2 \to m_1^2/2 - \delta_N$. Then, only the combination δ_S-δ_N appears in the mass formulas. Only this difference will be determined by the fit of the (axial-)vector masses. Alternately, we may set $\delta_N = 0$ from the beginning, and determine δ_S from the fit.

(iii) The parameters g_3, g_4, g_5, and g_6 do not influence any of the decays to be discussed in this work and are therefore not considered in the fit.

Consequently, we are left with the following 13 parameters:

$$m_0^2,\ m_1^2,\ c_1,\ \delta_S,\ g_1,\ g_2,\ h_{0N},\ h_{0S},\ h_1,\ h_2,\ h_3,\ \lambda_1,\ \lambda_2. \tag{36}$$

Their large-N_c dependence reads [15]

$$m_0^2,\ m_1^2,\ \delta_S \propto N_c^0;\ h_{0N},\ h_{0S} \propto N_c^{1/2};\ g_1,\ g_2 \propto N_c^{-1/2};\ \lambda_2,\ h_2,\ h_3 \propto N_c^{-1};\ \lambda_1,\ h_1 \propto N_c^{-2};\ c_1 \propto N_c^{-3}. \tag{37}$$

We recall that a nonsuppressed n-meson interaction vertex scales as $N_c^{1-n/2}$ [33]. In this respect the parameters h_1 and λ_1 are suppressed in the large-N_c limit: in fact, they scale as N_c^{-2} and not as N_c^{-1}. Similarly, the axial-anomaly

parameter c_1 scales as N_c^{-3} and not as N_c^{-2}. Note that the large-N_c behavior of the model parameters (37) implies that the decay widths (the formulas for which are given in Appendix B) decrease with increasing N_c. For this reason, as already mentioned, the states in our model represent $\bar{q}q$ states.

III. FIT: RESULTS AND CONSEQUENCES

A. Input and constraints for the fit

Let us now turn to the fit procedure for the parameters discussed above. Our fit aims to ascertain (i) whether it is possible to find a fit containing masses and decay widths for (pseudo)scalar and (axial-)vector degrees of freedom present in our model and (ii) which physical scalar states are best described by the $\bar{q}q$ states of our model.

All decays considered are two-particle decays; thus they can be calculated from the appropriate tree-level terms of the Lagrangian (2) after applying the necessary field shifts (10) and orthogonal transformations (A11). If the decaying particle is denoted by A and the decay products by B and C, respectively, the decay width reads

$$\Gamma_{A\to BC} = \mathcal{I}\frac{|\mathbf{k}|}{8\pi m_A^2}|\mathcal{M}_{A\to BC}|^2, \tag{38}$$

where $\mathbf{k}$ is the three-momentum of one of the resulting particles in the rest frame of A and $\mathcal{M}_{A\to BC}$ is the transition matrix element (decay amplitude). Moreover, $\mathcal{I}$ refers to the so-called isospin factor which is the number of subchannels in a given decay channel (for instance, if $B = C = K$ the $A \to KK$ decay can have two subchannels, namely K^+K^- and $\bar{K}^0K^0$, which results in $\mathcal{I} = 2$). Equation (38) will be used to calculate all decay widths entering the fit; details of the calculations can be found in Appendix B. Moreover, when identical particles emerge in the final state, the usual symmetry factors are included.

A brief remark is necessary regarding the errors used in the fit. The fit will contain input information from experimental data regarding both (axial-)vector and (pseudo) scalar states. The data are very precise for some of the resonances described by our model. For example, the mass of the $\phi(1020)$ resonance (our ω_S state) is known with 0.002% accuracy. Our model does not aim to describe hadron vacuum phenomenology with this extreme precision. The reason is simple: already isospin-breaking effects in the physical hadron mass spectrum are of the order of 5% [for instance the difference between the charged and neutral pion masses, or the masses of the $a_1(1260)$ and the $f_1(1285)$], but are completely neglected in our model. We therefore artificially increase the experimental errors to 5%, if the actual error is smaller, or we use the experimental values, if the error is larger than 5%.

Let us now discuss the input information for our fit. We do this separately for mesons of different spin (central values from PDG [1] unless otherwise stated, errors according to the above discussion):

(i) *Weak decay constants.* We use

$$\begin{aligned} f_\pi &= (92.2 \pm 4.6)\ \text{MeV}, \\ f_K &= (155.6/\sqrt{2} \pm 5.5)\ \text{MeV}. \end{aligned} \tag{39}$$

The following formulas relate the decay constants to the vacuum condensates: $f_\pi = \phi_N/Z_\pi$ and $f_K = (\sqrt{2}\phi_S + \phi_N)/(2Z_K)$.

(ii) *Pseudoscalar mesons.* We use

$$\begin{aligned} m_\pi &= (138 \pm 6.9)\ \text{MeV}, \\ m_K &= (495.6 \pm 24.8)\ \text{MeV}, \\ m_\eta &= (547.9 \pm 27.4)\ \text{MeV}, \\ m_{\eta'} &= (957.8 \pm 47.9)\ \text{MeV}, \end{aligned} \tag{40}$$

with the following notes: (i) m_π and m_K represent isospin-averaged values; (ii) the relatively large error values come from the criterion max(5%, experimental error), discussed above.

(iii) *Vector mesons.* We use

$$\begin{aligned} m_\rho &= (775.5 \pm 38.8)\ \text{MeV}, \\ m_{K^\star} &= (893.8 \pm 44.7)\ \text{MeV}, \\ m_\phi &= (1019.5 \pm 51)\ \text{MeV}, \\ \Gamma_{\rho\to\pi\pi} &= (149.1 \pm 7.4)\ \text{MeV}, \\ \Gamma_{K^\star\to K\pi} &= (46.2 \pm 2.3)\ \text{MeV}, \\ \Gamma_{\phi\to KK} &= (3.54 \pm 0.178)\ \text{MeV}, \end{aligned} \tag{41}$$

with the following notes: (i) we use the isospin-averaged value for $m_{K^\star}$; (ii) in case of the ϕ decay we use the physical mass values in the kinematic factor $k_K^3 = (m_\phi^2 - 4m_K^2)^{3/2}$ due to the proximity of $m_{\phi(1020)}$ to the $\bar{K}K$ threshold (in order to eliminate phase-space effects).

(iv) *Axial-vector mesons.* We use

$$\begin{aligned} m_{a_1} &= (1230 \pm 61.5)\ \text{MeV}, \\ m_{f_1(1420)} &= (1426.4 \pm 71.3)\ \text{MeV}, \\ \Gamma_{a_1\to\rho\pi} &= (425 \pm 175)\ \text{MeV}, \\ \Gamma_{a_1\to\pi\gamma} &= (0.640 \pm 0.250)\ \text{MeV}, \\ \Gamma_{f_1(1420)\to K^\star K} &= (43.9 \pm 2.2)\ \text{MeV}, \end{aligned} \tag{42}$$

with the following notes: (i) the value of $\Gamma_{a_1\to\rho\pi}$ is not precisely known; there are experimental data suggesting this decay channel to be dominant for a_1 [34] and thus we estimate the possible range for $\Gamma_{a_1\to\rho\pi}$ from the interval for the full a_1 decay width [= (250–600) MeV]; (ii) according to PDG the channel $f_1(1420) \to K^\star K$ is dominant within the channel $f_1(1420) \to KK\pi$, with the latter being

the overall dominant decay mode for $f_1(1420)$; we have assumed $\Gamma_{f_1(1420)\to KK\pi}$ to be equal to the full decay width $\Gamma_{f_1(1420)} = (54.9 \pm 2.6)$ MeV and determined $\Gamma_{f_1(1420)\to K^\star K}$ using an averaged branching ratio $\Gamma_{f_1(1420)\to K^\star K}/\Gamma_{f_1(1420)\to KK\pi} = (0.8 \pm 0.09)$ from Refs. [35,36].

(v) *Isotriplet and isodoublet scalar mesons.* The observables from Eqs. (40) to (42) will be used with any of the a_0-$K_0^\star$ combinations [$a_0(980)/K_0^\star(800)$, $a_0(980)/K_0^\star(1430)$, $a_0(1450)/K_0^\star(800)$, $a_0(1450)/K_0^\star(1430)$], where the data to be used are as follows:

$$\begin{aligned}
m_{a_0(980)} &= (980 \pm 49)\ \text{MeV},\\
m_{a_0(1450)} &= (1474 \pm 74)\ \text{MeV},\\
m_{K_0^\star(800)} &= (676 \pm 40)\ \text{MeV},\\
m_{K_0^\star(1430)} &= (1425 \pm 71)\ \text{MeV},\\
\Gamma_{a_0(1450)} &= (265 \pm 13.3)\ \text{MeV},\\
\Gamma_{K_0^\star(800)\to K\pi} &= (548 \pm 27.4)\ \text{MeV},\\
\Gamma_{K_0^\star(1430)\to K\pi} &= (270 \pm 80)\ \text{MeV},\\
|\mathcal{M}_{a_0(980)\to KK}| &= (3590 \pm 440)\ \text{MeV}\,[37],\\
|\mathcal{M}_{a_0(980)\to \eta\pi}| &= (3300 \pm 166.5)\ \text{MeV}\,[37].
\end{aligned} \tag{43}$$

We note the following: (i) the interpretation of $K_0^\star(800)$ as a particle is controversial; we will nonetheless include it into our fits in accordance with the conclusions of Ref. [4]; (ii) as in the case of $\phi(1020)$, we will use the decay amplitudes rather than the decay widths for the processes $a_0(980) \to KK$ and $a_0(980) \to \eta\pi$ due to the proximity of $a_0(980)$ to the $\bar{K}K$ threshold. The reader may find it somewhat surprising that we are considering pairs of states above [$a_0(1450)/K_0^\star(1430)$] 1 GeV, below [$a_0(980)/K_0^\star(800)$] 1 GeV, as well as "mixed" pairs $a_0(980)/K_0^\star(1430)$, $a_0(1450)/K_0^\star(800)$. The reason to consider also mixed pairs is that we want to avoid any kind of prejudice in the assignment of our $\bar{q}q$ states, and thus explore all possibilities. Nonetheless, these mixed pairs as well as the pair below 1 GeV will be disfavored by our analysis (see below). Mass formulas used in the fit are presented in Eqs. (15)–(18), (20)–(23), and (25)–(34), whereas formulas for the decay widths are given in Appendix B.

Moreover, the fit shall be constrained by the following conditions:

(i) $Z_\pi, Z_K, Z_{\eta_S}, Z_{K_0^\star} > 1$, due to Eqs. (13) and (14).

(ii) $m_{\eta_N} < m_{\eta_S}$ and $m_{\sigma_N} < m_{\sigma_S}$, i.e., pure nonstrange states should be lighter than pure strange states.

(iii) $m_0^2 < 0$. This is a necessary condition for the spontaneous breaking of chiral symmetry.

(iv) $\lambda_2 > 0$ and $\lambda_1 > -\lambda_2/2$. This is necessary for the potential in the Lagrangian (2) to be bounded from below.

(v) $m_1^2 \geq 0$. The reason is that otherwise (i) an instability of the vacuum in the physical ρ direction would occur [see the Lagrangian (2)] and (ii) m_ρ and m_{a_1} would become imaginary in the chiral transition, i.e., once the condensates vanish [see Eqs. (27) and (31)].

(vi) $m_1 \leq m_\rho$ as otherwise $(h_1 + h_2 + h_3)\phi_N^2/2 + h_1\phi_S^2/2$ in the ρ mass term (27) would be negative; this would imply that spontaneous chiral symmetry breaking decreases the ρ mass. This is clearly unnatural because the breaking of chiral symmetry generates a sizable constituent mass for the light quarks, which is expected to positively contribute to the meson masses. This positive contribution is a feature of all known models (such as the Nambu-Jona-Lasinio model and constituent quark approaches). Indeed, in an important class of hadronic models (see Ref. [38] and references therein) the only and obviously positive contribution to the ρ mass squared is proportional to ϕ^2 (i.e., $m_1 = 0$).

Before discussing the results of the fit, it is important to stress which particles have not been included in the list above and why. Namely, we have omitted experimental information about the scalar-isoscalar and the axial-kaon states.

(i) Scalar-isoscalar states are not included in the fit because in this first study we have neglected the coupling of the glueball and of additional light scalar states, such as tetraquarks, to the other mesons. Thus, although there are three scalar states [28] above 1 GeV, at most two can be described within our model. Below 1 GeV the resonance $f_0(500)$ is still poorly known and $f_0(980)$ is distorted by the nearby $\bar{K}K$ threshold.

(ii) The axial-kaon state K_1 is not included in the fit for a similar reason: the kaonic states from our axial-vector nonet 1^{++} mix with the kaonic states of the nonet 1^{+-} which is not part of our Lagrangian. (This is possible, because charge conjugation is not a well-defined quantum number for kaons.) Also in this case we cannot assign our theoretical axial-kaon field to a specific resonance [in PDG there are two axial kaons with masses $K_1(1270)$ and $K_1(1400)$], because the mixing is expected to be large (see, e.g., Ref. [39]).

B. Results of the fit

The experimental quantities discussed in the previous subsection do not depend on all 13 parameters of Eq. (36), but on m_0, λ_1, m_1, h_1 only through the two combinations

$$\begin{aligned}
C_1 &= m_0^2 + \lambda_1(\phi_N^2 + \phi_S^2),\\
C_2 &= m_1^2 + \frac{h_1}{2}(\phi_N^2 + \phi_S^2).
\end{aligned} \tag{44}$$

Moreover, instead of the parameters h_{0N} and h_{0S} we use the condensates ϕ_N and ϕ_S: this is equivalent, as h_{0N}, h_{0S} are completely determined by the masses of pion and η_S; cf. Eqs. (15) and (18). Summarizing, we have the following 11 parameters entering the fit:

$$C_1, C_2, c_1, \delta_S, g_1, g_2, \phi_N, \phi_S, h_2, h_3, \lambda_2. \tag{45}$$

We perform our fit using the experimental values for the 17 quantities given in Eqs. (39)–(42). In addition, we use the experimental values for the pairs $a_0(980)/K_0^\star(800)$, $a_0(980)/K_0^\star(1430)$, $a_0(1450)/K_0^\star(800)$, $a_0(1450)/K_0^\star(1430)$ given in Eq. (43). These are four additional experimental quantities [except in the case of $a_0(980)$, where we use the two values for the decay amplitudes instead of one value for the decay width]. In total, we therefore fit 21 (or 22) experimental quantities to the 11 parameters given in Eq. (45). The corresponding values of χ^2 are listed in Table I. We see that the combination $a_0(1450)/K_0^\star(1430)$ gives the best value for χ^2. In fact, with a $\chi^2_{\rm red}$ of 1.23 this fit is remarkably good, meaning that all physical quantities are reproduced within an average error of 5%. In the framework of an effective model for the strong interaction, which neglects isospin-breaking effects and describes all mesonic resonances up to about 1.8 GeV, we perceive this to be a remarkable achievement.

Note that also the fit with the pair $a_0(980)/K_0^\star(1430)$ has a $\chi^2_{\rm red}$ of the same order of magnitude as the one with the pair $a_0(1450)/K_0^\star(1430)$. Nevertheless, we will disregard this fit for two reasons. First, the $\chi^2_{\rm red}$ for the pair $a_0(980)/K_0^\star(1430)$ is, although rather small, still larger by a factor of about 2 than the $\chi^2_{\rm red}$ for the pair $a_0(1450)/K_0^\star(1430)$. Second, and more importantly, the fit with the pair $a_0(980)/K_0^\star(1430)$ produces a scalar-kaon mass of $m_{K_0^\star} = 1146$ MeV, which cannot be assigned to any physical resonance as it is much larger than $m_{K_0^\star(800)}$ and much smaller than $m_{K_0^\star(1430)}$. Note that this problem is also present in Nambu-Jona-Lasinio models with mixing between scalar mesons below and above 1 GeV [40].

The detailed comparison of theory with data for the pair $a_0(1450)/K_0^\star(1430)$ is presented in Table II where the theoretical errors are also shown. Errors for the model parameters (δp_i) are calculated as the inverse square roots of the eigenvalues of the Hessian matrix obtained from $\chi^2(p_j)$, where p_j denotes elements of the parameter set (45) and $i = 1, 2, \ldots, 11$. Theoretical errors ΔO_i for each observable O_i (mass, decay width) can be calculated according to the following formula:

$$\Delta O_i = \sqrt{\sum_{j=1}^{n} \left(\frac{\partial O_i}{\partial p_j} \bigg|_{\text{at fit value of } O_i} \delta p_j \right)^2}. \tag{46}$$

The remarkable agreement of our results with experimental data in the (pseudo)scalar and (axial-)vector sectors can now be explicitly seen for the various quantities shown in Table II. We thus conclude that the quark-antiquark states a_0 and K_0^* should be assigned to the resonances $a_0(1450)$ and $K_0^*(1450)$. Moreover, also the axial-vector resonances are well described by the fit: we therefore also interpret them as predominantly quark-antiquark states.

In Fig. 1 we present the results of Table II in a slightly different way: as the difference of the theoretical and experimental values divided by experimental error—the error bars correspond to the theoretical error values from our fit.

In Table III we finally present the values of the parameters of the model together with their errors as obtained from our best fit. We remark that, since the quantities entering our fit are not affected by interactions with the glueball, this result holds also when including the latter.

Before moving to the consequences of the fit, we discuss two important aspects of our study:

TABLE I. Isotriplet and isodoublet scalar pairs and the corresponding values of the total χ^2 and the reduced $\chi^2_{\rm red} = \chi^2/N_{\rm dof}$, where $N_{\rm dof}$ is the difference between the number of experimental quantities and the number of fit parameters (10 for the first and fourth rows and 11 for the second and third rows).

Pair	χ^2	$\chi^2_{\rm red}$
$a_0(1450)/K_0^\star(1430)$	12.33	1.23
$a_0(980)/K_0^\star(800)$	129.36	11.76
$a_0(980)/K_0^\star(1430)$	22.00	2.00
$a_0(1450)/K_0^\star(800)$	242.27	24.23

TABLE II. Best-fit results for masses and decay widths compared with experiment.

Observable	Fit (MeV)	Experiment (MeV)
f_π	96.3 ± 0.7	92.2 ± 4.6
f_K	106.9 ± 0.6	110.4 ± 5.5
m_π	141.0 ± 5.8	137.3 ± 6.9
m_K	485.6 ± 3.0	495.6 ± 24.8
m_η	509.4 ± 3.0	547.9 ± 27.4
$m_{\eta'}$	962.5 ± 5.6	957.8 ± 47.9
m_ρ	783.1 ± 7.0	775.5 ± 38.8
$m_{K^\star}$	885.1 ± 6.3	893.8 ± 44.7
m_ϕ	975.1 ± 6.4	1019.5 ± 51.0
m_{a_1}	1186 ± 6	1230 ± 62
$m_{f_1(1420)}$	1372.5 ± 5.3	1426.4 ± 71.3
m_{a_0}	1363 ± 1	1474 ± 74
$m_{K_0^\star}$	1450 ± 1	1425 ± 71
$\Gamma_{\rho\to\pi\pi}$	160.9 ± 4.4	149.1 ± 7.4
$\Gamma_{K^\star\to K\pi}$	44.6 ± 1.9	46.2 ± 2.3
$\Gamma_{\phi\to\bar{K}K}$	3.34 ± 0.14	3.54 ± 0.18
$\Gamma_{a_1\to\rho\pi}$	549 ± 43	425 ± 175
$\Gamma_{a_1\to\pi\gamma}$	0.66 ± 0.01	0.64 ± 0.25
$\Gamma_{f_1(1420)\to K^\star K}$	44.6 ± 39.9	43.9 ± 2.2
Γ_{a_0}	266 ± 12	265 ± 13
$\Gamma_{K_0^\star\to K\pi}$	285 ± 12	270 ± 80

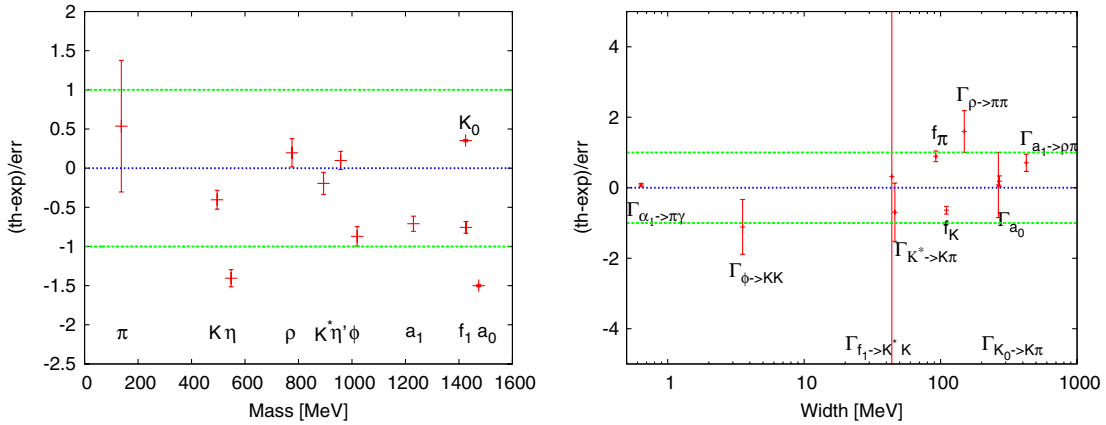

FIG. 1 (color online). Comparison of theory and experiment for observables from Table II.

(i) *Mass ordering in the scalar sector.* As evident from Table II, our fit yields $m_{a_0} < m_{K_0^\star}$ whereas the experimental mass ordering is opposite. The reason for our result is the pattern of explicit symmetry breaking implemented in our model, which renders $\bar{q}q$ states with a strange quark approximately 100 MeV heavier than nonstrange states. However, other mechanisms, as for instance mixing of the currently present $\bar{q}q$ states with light tetraquark states, may occur that change this mass ordering [41–43]: namely, in this mixing scenario a pure quarkonium and a pure tetraquark in the isovector sector mix to form the resonances $a_0(1450)$ and $a_0(980)$, while a similar mixing in the isodoublet sector leads to the resonances $K_0^*(1450)$ and $K_0^*(800)$. The fact that the mass ordering $m_{a_0} > m_{K_0^\star}$ is realized in nature can be understood from a larger mixing angle, and therefore a larger level repulsion, in the isovector sector. A detailed study of this scenario necessitates the inclusion of a full nonet of light states (see also the discussion in the Conclusions).

An additional point can be raised about the ratio of the full decay widths of the $a_0(1450)$ and $K_0^\star(1430)$ resonances. From $SU(3)_V$ symmetry arguments for $\bar{q}q$ states one expects the full decay widths of these resonances to scale as [41]

$$\frac{\Gamma_{a_0(1450)}}{\Gamma_{K_0^\star(1430)}} = 1.51 \tag{47}$$

whereas experimental data suggest [1]

$$\frac{\Gamma_{a_0(1450)}}{\Gamma_{K_0^\star(1430)}} \sim 0.9. \tag{48}$$

In Ref. [41], this problem was also solved by introducing tetraquark fields at the level of an effective Lagrangian and by studying tetraquark-quarkonium mixing in the $I = 1$ and $I = 1/2$ channels. Contrarily, in our considerations so far only $\bar{q}q$ states were taken into account. Thus one might expect that our fit results should be closer to the $SU(3)$ limit rather than to the experimental ratio. However, the opposite is the case: as evident from Table II, our fit results for $a_0(1450)$ and $K_0^\star(1430)$ reproduce the experimental ratio $\sim$0.9. Our analysis shows that the reason is the inclusion of the chiral-anomaly term and, in particular, of (axial-)vector mesons. Artificially decoupling (axial-)vector states (i.e., setting $g_1 = h_2 = h_3 = 0$) and removing the chiral-anomaly term from our Lagrangian (i.e., setting $c_1 = 0$) we obtain unphysically large decay widths $\Gamma_{a_0(1450)} \sim 14$ GeV, $\Gamma_{K_0^\star(1430)} \sim 10$ GeV—and also $\Gamma_{a_0(1450)}/\Gamma_{K_0^\star(1430)} \sim 1.4$, very close to the value obtained from $SU(3)$ symmetry. The ratio would be $\sim$1.3 if only (axial-)vectors were decoupled. Hence, just as in our previous publication [15], we emphasize again the crucial importance of the (axial-)vector degrees of freedom for scalar-meson phenomenology. However, there still remains an open question how additional light scalar fields will influence the results in the a_0-$K_0^\star$ sector.

(ii) *Unitarity corrections.* Our results for masses and decay widths are valid at tree level. Most particles in

TABLE III. Parameters and their errors.

Parameter	Value
C_1 [GeV^2]	-0.9183 ± 0.0006
C_2 [GeV^2]	0.4135 ± 0.0147
c_1 [GeV^{-2}]	450.5420 ± 7.0339
δ_S [GeV^2]	0.1511 ± 0.0038
g_1	5.8433 ± 0.0176
g_2	3.0250 ± 0.2329
ϕ_N [GeV]	0.1646 ± 0.0001
ϕ_S [GeV]	0.1262 ± 0.0001
h_2	9.8796 ± 0.6627
h_3	4.8667 ± 0.0864
λ_2	68.2972 ± 0.0435

our model are rather narrow, and thus justify—at least in a first approximation—this procedure. This is also in agreement with large-N_c considerations, according to which the role of the contribution of mesonic loops is suppressed. However, the axial-vector state $a_1(1230)$ and the scalar states $a_0(1450)$ and $K_0^\star(1430)$, as well as the scalar-isoscalar state $f_0(1370)$ to be discussed in the next subsection, have a large width (of the order of 300 MeV or more). Then, the role of loops and unitarity corrections for both the masses and the decay widths needs to be discussed. Concerning the mass shifts due to mesonic loops, we notice that an indirect indication that their contribution is not too large is the fact that the resonances $a_1(1260)$ and $f_1(1285)$ have a similar mass, although the former has a much larger decay width than the latter. In a theoretical study of this system one should determine the pole position of the resonance: the mass is then usually denoted as the real part of the pole. As shown recently in Ref. [44], the value of the real part of the pole does not differ too much from the bare (tree-level) mass, not even for large coupling constants. Concerning the influence of loops on the value of decay widths, we note that Ref. [45] has shown that the corrections are small as long as the ratio Γ/m is small. For instance, for the case of $f_0(1370)$, the average decay width reported by the Particle Data Group is 350 MeV whereas the average resonance mass is 1350 MeV. This implies $\Gamma/m \sim 0.26$. The ratio is almost as small as in the case of the ρ meson where $\Gamma/m \sim 150/750 = 0.2$—and it is known from chiral perturbation theory that such resonances obtain only small corrections upon unitarizations (see, e.g., Ref. [46]).

We thus conclude that the role of loops should not modify the picture presented here. It should, however, be stressed that the inclusion of loops is a necessary step for the future: on the one hand we can numerically evaluate the role of mesonic loops and thus quantitatively verify our statements; on the other hand, even if large variations for the states above 1 GeV do not occur as we expect, an interesting question is how poles on the complex plane emerge. Namely, these states could arise as tetraquark states as mentioned above, but could also represent dynamically generated states (see also, e.g., Ref. [47]). (For a detailed discussion of this point including the interrelations of tetraquark, molecular, and dynamically generated states we refer to Ref. [31].)

C. Consequences of the fit

1. Scalar-isoscalar mesons

We now turn to the scalar-isoscalar mesons. We shall discuss four different aspects:

(a) Results in the large-N_c limit ($\lambda_1 = h_1 = 0$). From the fit in the previous section we cannot immediately obtain the masses of the scalar-isoscalar states of the model because their masses do not depend solely on the combination $C_1 = m_0^2 + \lambda_1(\phi_N^2 + \phi_S^2)$, but separately on the parameters m_0^2 and λ_1. Similarly, the decay rates of the scalar-isoscalar mesons do not depend solely on the combination $C_2 = m_1^2 + \frac{h_1}{2}(\phi_N^2 + \phi_S^2)$, but separately on the parameters m_1 and h_1.
Interestingly, the parameters λ_1 and h_1 are large-N_c suppressed. Setting them to zero we obtain a prediction for the masses and decay widths of the scalar-isoscalar states in the large-N_c limit. Moreover, when $\lambda_1 = h_1 = 0$, there is also no mixing between $\bar{n}n$ and $\bar{s}s$ states: $f_0^L \equiv \sigma_N = \bar{n}n \equiv (\bar{u}u + \bar{d}d)/\sqrt{2}$ and $f_0^H \equiv \sigma_S \equiv \bar{s}s$. Their masses read

$$m_{f_0^L} = 1362.7 \text{ MeV}, \qquad m_{f_0^H} = 1531.7 \text{ MeV}. \tag{49}$$

These masses clearly lie above 1 GeV. Comparing these values to the experimental values for the three isoscalar states above 1 GeV [1],

$$\begin{aligned} m_{f_0(1370)} &= (1350 \pm 150) \text{ MeV}, \\ m_{f_0(1500)} &= (1505 \pm 75) \text{ MeV}, \\ m_{f_0(1710)} &= (1720 \pm 86) \text{ MeV}, \end{aligned} \tag{50}$$

we see that the mass of f_0^L is well compatible with that of the resonance $f_0(1370)$. [Note that $m_{f_0(1370)}$ in Eq. (50) emulates the PDG mass interval (1200–1500) MeV.] The mass of f_0^H appears to be close to that of $f_0(1500)$. Remember, though, that we artificially enlarged the experimental error to 5%; the actual error is only 6 MeV, and then the mass of f_0^H would be (just) outside the experimental error. Considering the decays of f_0^H we shall provide evidence that an assignment of f_0^H to $f_0(1710)$ is also possible (and even rather likely).
For $\lambda_1 = h_1 = 0$ the decay rates of $f_0^{L,H}$ into $\pi\pi$ and KK read

$$\Gamma_{f_0^L \to \pi\pi} = 520 \text{ MeV}, \qquad \Gamma_{f_0^L \to KK} = 129 \text{ MeV}, \tag{51}$$

$$\Gamma_{f_0^H \to \pi\pi} = 0 \text{ MeV}, \qquad \Gamma_{f_0^H \to KK} = 422 \text{ MeV}. \tag{52}$$

For the experimental values we quote the PDG values [1]:

$$\begin{aligned}
\Gamma_{f_0(1370)\to\pi\pi} &= (250 \pm 100)\ \text{MeV},\\
\Gamma_{f_0(1370)\to KK} &\lesssim \Gamma_{f_0(1370)\to\pi\pi},\\
\Gamma_{f_0(1500)\to\pi\pi} &= (38 \pm 5)\ \text{MeV},\\
\Gamma_{f_0(1500)\to KK} &= (9.4 \pm 2.3)\ \text{MeV},\\
\Gamma_{f_0(1710)\to\pi\pi} &= (29.3 \pm 6.5)\ \text{MeV},\\
\Gamma_{f_0(1710)\to KK} &= (71.4 \pm 29.1)\ \text{MeV}.
\end{aligned} \tag{53}$$

Note that for the resonance $f_0(1370)$ no branching ratios into $\pi\pi$ and KK are reported in Ref. [1]. The value for $\Gamma_{f_0(1370)\to\pi\pi}$ is our estimate from PDG and the review [7], whereas $\Gamma_{f_0(1370)\to KK}$ is our estimate from results presented in Refs. [1,48].

Our results for f_0^L are in agreement with the experimental decay widths of $f_0(1370)$. Our theoretical value for $f_0^H \to KK$ turns out to be too large, while $f_0^H \to \pi\pi$ vanishes, because $f_0^H \equiv \sigma_S$ is a pure $\bar{s}s$ state. Nevertheless, our model predicts the existence of a scalar-isoscalar state which decays predominantly into kaons; this is indeed the decay pattern shown by $f_0(1710)$. For these reasons we suggest to identify our state f_0^H as (predominantly) $f_0(1710)$. This identification will be further tested when $\lambda_1 \neq 0$, $h_1 \neq 0$ below.

It should be stressed that a quantitative study of the scalar-isoscalar system cannot be performed at present because our model contains only two states, while three resonances appear (this is also the reason why we did not include the scalar-isoscalar states into the fit). As many studies confirm [28], the mixing with the scalar glueball can be sizable: a reliable analysis of the scalar-isoscalar states can only be performed when taking the scalar glueball into account. The preliminary results in the $N_f = 2$ sector [24] have indeed shown that the glueball and quarkonia degrees of freedom interact strongly and that the decay patterns are sizably influenced.

(b) Results for $\lambda_1 \neq 0$, $h_1 \neq 0$.

A nonvanishing value of the parameter λ_1 induces a mixing of the pure states σ_N and σ_S [see Eq. (24)]. Our fit determines only the value of the linear combination C_1 rather than the value of λ_1 [see discussion before Eq. (45)]. Nonetheless, a range of values for λ_1 can be estimated using the value of C_1 from the fit and the condition $m_0^2 < 0$. Consequently, we also obtain a range of values for our isoscalar masses $m_{f_0^{L,H}}$ and isoscalar decay widths. The masses vary in the following intervals: 415 MeV $\lesssim m_{f_0^L} \lesssim$ 1460 MeV and 1480 MeV $\lesssim m_{f_0^H} \lesssim$ 1981 MeV. Considering these mass values, f_0^L may correspond to either $f_0(500)$, $f_0(980)$, or $f_0(1370)$ and f_0^H may correspond to either $f_0(1500)$ or $f_0(1710)$ [1]. Therefore, a mere calculation of scalar masses does not allow us to assign the scalar states f_0^L and f_0^H to physical resonances. In order to resolve this ambiguity, we will calculate various decay widths of the states f_0^L and f_0^H and compare them to data [1].

The dependence of $\Gamma_{f_0^{L,H}\to\pi\pi}$ on $m_{f_0^{L,H}}$ is presented in Fig. 2.

The decay width $\Gamma_{f_0^L\to\pi\pi}$ is consistent with the experimental range (250 ± 100) MeV for the $f_0(1370) \to \pi\pi$ decay width, if 1000 MeV $\lesssim m_{f_0^L} \lesssim$ 1460 MeV. Other assignments can be excluded: (i) Our f_0^L state cannot be assigned to $f_0(500)$ as $\Gamma_{f_0^L\to\pi\pi} \lesssim 20$ MeV in the (new) PDG mass range (400–550) MeV for $f_0(500)$. Therefore, this strongly disfavors $f_0(500)$ as a $\bar{q}q$ state. (ii) $\Gamma_{f_0^L\to\pi\pi}$ varies between approximately 140 MeV and 170 MeV in the mass interval of the $f_0(980)$ resonance; i.e., the interval between 970 MeV and 1010 MeV. The PDG result for the full decay width of the $f_0(980)$ resonance is between 40 MeV and 100 MeV, with the $\pi\pi$ channel being dominant [1], i.e., about a factor 2 smaller than our theoretical values. Consequently, the assignment of f_0^L to $f_0(980)$ is also disfavored by our analysis. Therefore (although there could still be mixing with other states) we assign our f_0^L state to $f_0(1370)$, thus supporting the interpretation of the latter state as a quarkonium. Although experimental

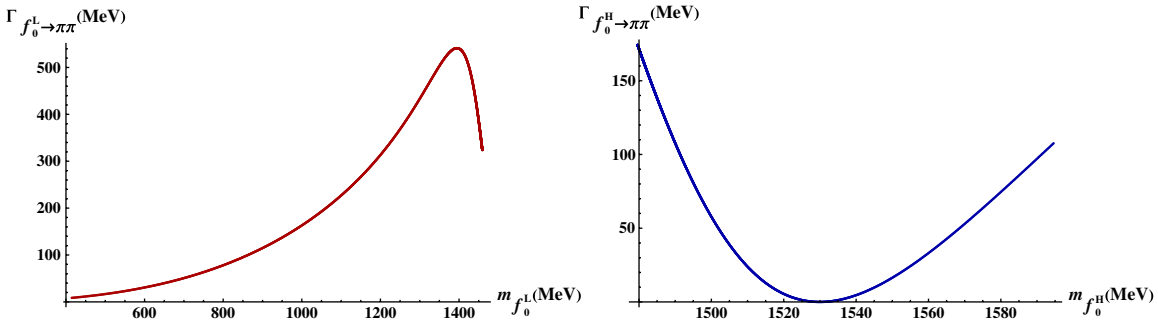

FIG. 2 (color online). $\Gamma_{f_0^L\to\pi\pi}$ and $\Gamma_{f_0^H\to\pi\pi}$ as functions of $m_{f_0^L}$ and $m_{f_0^H}$, respectively.

data are not conclusive, we mention that the decay width $\Gamma_{f_0^L\to KK}$ shown in Fig. 3 is consistent with the data.

In the mass interval $1500\ \text{MeV} \lesssim f_0^H \lesssim 1560\ \text{MeV}$, our results for the decay width $\Gamma_{f_0^H\to\pi\pi}$ are consistent with experimental values for both $f_0(1500)$ and $f_0(1710)$ [see Eq. (53)]. However, the KK decay widths present us with a different conclusion: as already indicated in the case $\lambda_1 = h_1 = 0$, our f_0^H state decays much more abundantly into kaons than into pions, and the experimental data suggest only one physical resonance with the same feature, $f_0(1710)$. The other resonance $f_0(1500)$ decays preferably into pions. Thus (and although the mass value for f_0^H is too small in the range where the decay width into pions agrees with the experimental value) we assign our f_0^H state to $f_0(1710)$ and inspect in the following whether this assignment is justified by other data.

We observe from Fig. 3 that $\Gamma_{f_0^H\to KK}$ rises rapidly and remains above the PDG result $\Gamma_{f_0(1710)\to KK} = (71.4 \pm 29.1)\ \text{MeV}$ in the entire mass interval $m_{f_0^H} \gtrsim 1500\ \text{MeV}$. Although the absolute value of the decay width is rather large, several ratios of decay widths can be described correctly by our fit, most notably the $\pi\pi/KK$ decay ratio presented in Fig. 4.

Let us first discuss results for $\Gamma_{f_0^L\to KK}/\Gamma_{f_0^L\to\pi\pi}$ (left panel of Fig. 4). We observe that the ratio varies between 0.49 for $m_{f_0^L} = 1152\ \text{MeV}$ and 0 for $m_{f_0^L} = 1444\ \text{MeV}$. Experimental data regarding this ratio for $f_0(1370)$ are unfortunately inconclusive: $\Gamma_{f_0(1370)\to KK}/\Gamma_{f_0(1370)\to\pi\pi} = 0.08 \pm 0.08$ is quoted by the BESII Collaboration [49] and $\Gamma_{f_0(1370)\to KK}/\Gamma_{f_0(1370)\to\pi\pi} = 0.91 \pm 0.20$ is the value given by the OBELIX Collaboration [50]; for the mass interval shown in Fig. 4, our result is most consistent with the value of the WA102 Collaboration [51], $\Gamma_{f_0(1370)\to KK}/\Gamma_{f_0(1370)\to\pi\pi} = 0.46 \pm 0.15 \pm 0.11$. The ambiguities in the experimental value of this ratio do not allow us to constrain our parameters, although our f_0^L state is compatible with the $f_0(1370)$ data also for this particular case.

Let us now discuss results for $\Gamma_{f_0^H\to\pi\pi}/\Gamma_{f_0^H\to KK}$ (right panel of Fig. 4). As already mentioned, the analysis of the two-pion decay did not allow for a definitive assignment of our f_0^H state, as it could correspond either to $f_0(1500)$ or to $f_0(1710)$. The PDG data suggest the ratio $\Gamma_{f_0(1500)\to KK}/\Gamma_{f_0(1500)\to\pi\pi} = 0.246 \pm 0.026$ or $\Gamma_{f_0(1500)\to\pi\pi}/\Gamma_{f_0(1500)\to KK} = 4.065 \pm 0.430$, respectively, whereas, for $f_0(1710)$, we use the WA102 ratio $\Gamma_{f_0(1710)\to\pi\pi}/\Gamma_{f_0(1710)\to KK} = 0.2 \pm 0.06$ [51]. The latter is only marginally consistent with the one preferred by the PDG ($\Gamma^{\text{PDG}}_{f_0(1710)\to\pi\pi}/\Gamma^{\text{PDG}}_{f_0(1710)\to KK} = 0.41^{+0.11}_{-0.17}$), originally published by the BESII Collaboration [52], that suffers from a large background in the $\pi^+\pi^-$ channel (approximately 50%) and is therefore omitted from our considerations. We observe from the right panel of Fig. 4 that our ratio $\Gamma_{f_0^H\to\pi\pi}/\Gamma_{f_0^H\to KK}$ never corresponds to the one experimentally determined for $f_0(1500)$. Although the ratio shows a strong increase near the left border of the mass interval, decreasing the mass beyond this border would violate the constraint $m_0^2 < 0$. Thus, the experimental value is out of reach. Conversely, our ratio describes exactly the value $\Gamma_{f_0(1710)\to\pi\pi}/\Gamma_{f_0(1710)\to KK} = 0.2 \pm 0.06$ if $m_{f_0^H} = 1502^{-2}_{+3}\ \text{MeV}$. [We discard the second possibility $m_{f_0^H} = 1611^{+27}_{-23}\ \text{MeV}$ as the decay width $\Gamma_{f_0^H\to KK}$ would exceed 600 MeV (see Fig. 3), i.e., an order of magnitude larger than the experimental value [see Eq. (53)].] This implies $\lambda_1 = -4.1 \mp 0.7$—the parameter λ_1 remains close to the large-N_c limit and is much smaller than λ_2 (see Table III).

The contribution of the pure strange state σ_S to f_0^H is then approximately 96%, as can be calculated from Eqs. (A12)–(A16). Thus our predominantly strange state f_0^H describes the $\pi\pi/KK$ ratio of $f_0(1710)$, and not that of $f_0(1500)$, although the correct

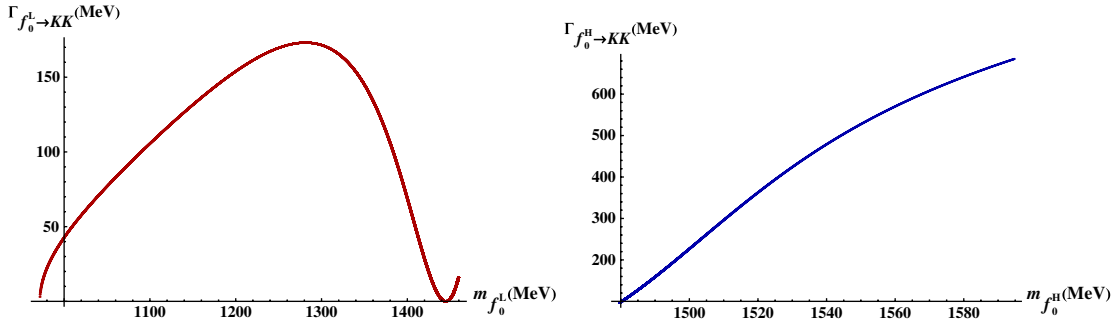

FIG. 3 (color online). $\Gamma_{f_0^L\to KK}$ and $\Gamma_{f_0^H\to KK}$ as functions of $m_{f_0^L}$ and $m_{f_0^H}$, respectively.

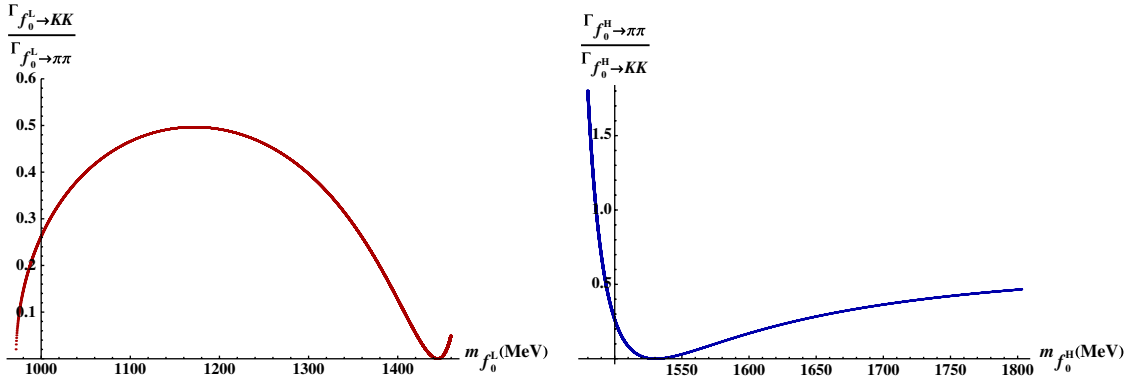

FIG. 4 (color online). Left panel: ratio $\Gamma_{f_0^L\to KK}/\Gamma_{f_0^L\to\pi\pi}$ as function of $m_{f_0^L}$. Right panel: ratio $\Gamma_{f_0^H\to\pi\pi}/\Gamma_{f_0^H\to KK}$ as function of $m_{f_0^H}$.

description requires that $m_{f_0^H}$ corresponds to the mass value of $f_0(1500)$. The correct description of the decay ratio is an indication that our assignment of f_0^H to $f_0(1710)$ is the correct one, whereas the fact that $m_{f_0^H}$ is smaller than $m_{f_0(1710)}$ indicates the necessity to include the coupling to the third isoscalar degree of freedom of our model: the glueball. As concluded from the $N_f = 2$ version of our model [24], the $f_0(1500)$ is predominantly a glueball state and thus considering the glueball state is expected to induce a level repulsion in the masses. This may shift the currently too small mass value of the predominantly strange quarkonium from approximately 1.5 GeV to 1.7 GeV, where it is experimentally found. Nonetheless, our results clearly demonstrate that scalar quarkonia are found above, rather than below, 1 GeV.

Until now we have only considered the case where one of our large-N_c suppressed parameters (λ_1) is nonzero. We have also investigated the influence of nonvanishing values for the other large-N_c suppressed parameter, h_1, on the decay widths $\Gamma_{f_0^{L,H}\to\pi\pi}$ and $\Gamma_{f_0^{L,H}\to KK}$ [see Eqs. (B24), (B25), (B30), and (B31)]. Consistency with the large-N_c deliberations requires us to keep h_1 smaller than, or in the vicinity of, h_2 and h_3 (see Table III). We again observe that our ratio $\Gamma_{f_0^H\to\pi\pi}/\Gamma_{f_0^H\to KK}$ never corresponds to the one of the $f_0(1500)$ resonance whereas the ratio $\Gamma_{f_0(1710)\to\pi\pi}/\Gamma_{f_0(1710)\to KK} = 0.2 \pm 0.06$ is correctly described if $h_1 \sim -9$. In this case, $m_{f_0^H}$ rises to approximately 1540 MeV and is thus outside the PDG result $m_{f_0(1500)} = (1505 \pm 6)$ MeV but still too small when compared to $m_{f_0(1710)} = (1720 \pm 6)$ MeV. Thus, it is still necessary to include a glueball degree of freedom into our model. Nonetheless, the qualitative correspondence of our predominantly nonstrange quarkonium to $f_0(1370)$ and of our predominantly strange quarkonium to $f_0(1710)$, and also the conclusion that scalar $\bar{q}q$ states are located in the energy region above 1 GeV, remain valid in the case $\lambda_1 \neq 0 \neq h_1$.

The assignment of f_0^H to $f_0(1710)$ is further justified considering decays into η and η' mesons.

(c) $\eta\eta$ and $\eta\eta'$ decay channels for the scalar-isoscalar mesons.

PDG data suggest the following values of $\eta\eta$ decay widths for $f_0(1500)$ and $f_0(1710)$ [1]:

$$\begin{aligned}\Gamma_{f_0(1500)\to\eta\eta} &= (5.56 \pm 1.34)\ \text{MeV},\\ \Gamma_{f_0(1710)\to\eta\eta} &= (38.6 \pm 18.8)\ \text{MeV}.\end{aligned} \tag{54}$$

Our analysis always yields $\Gamma_{f_0^H\to\eta\eta} > 20$ MeV; there is consequently no value of $m_{f_0^H}$ at which $\Gamma_{f_0^H\to\eta\eta}$ would be compatible with $\Gamma_{f_0(1500)\to\eta\eta}$. However, $m_{f_0^H} = 1502^{-2}_{+3}$ MeV (obtained requiring $\Gamma_{f_0^H\to\pi\pi}/\Gamma_{f_0^H\to KK} = \Gamma_{f_0(1710)\to\pi\pi}/\Gamma_{f_0(1710)\to KK}$, i.e., $\lambda_1 = -4.1 \mp 0.7$ and $h_1 = 0$) yields

$$\Gamma_{f_0^H\to\eta\eta} = 49.6^{+4.1}_{-3.3}\ \text{MeV} \tag{55}$$

(where the errors arise from the uncertainty in λ_1 only), i.e., in agreement with the experimental value for $f_0(1710)$ quoted in Eq. (54). The same parameter set also yields

$$\Gamma_{f_0^L\to\eta\eta} \simeq 33\ \text{MeV}, \tag{56}$$

which is purely a prediction, as $\Gamma_{f_0(1370)\to\eta\eta}$ has not yet been measured.

The choice $\lambda_1 = -4.1 \mp 0.7$, $h_1 = 0$ also yields

$$\begin{aligned}\Gamma_{f_0^L\to\eta\eta}/\Gamma_{f_0^L\to KK} &= 0.194^{+0.002}_{-0.003},\\ \Gamma_{f_0^H\to\eta\eta}/\Gamma_{f_0^H\to KK} &= 0.204^{+0.001}_{-0.002},\end{aligned} \tag{57}$$

$$\begin{aligned}\Gamma_{f_0^L\to\eta\eta}/\Gamma_{f_0^L\to\pi\pi} &= 0.087^{+0.005}_{-0.006},\\ \Gamma_{f_0^H\to\eta\eta}/\Gamma_{f_0^H\to\pi\pi} &= 1.02^{-0.23}_{+0.42},\end{aligned} \tag{58}$$

whereas experimental data read

$$\Gamma_{f_0(1500)\to\eta\eta}/\Gamma_{f_0(1500)\to KK} = 0.59 \pm 0.12 \quad [1], \tag{59}$$

$$\Gamma_{f_0(1500)\to\eta\eta}/\Gamma_{f_0(1500)\to\pi\pi} = 0.145 \pm 0.027 \quad [1], \tag{60}$$

$$\Gamma_{f_0(1710)\to\eta\eta}/\Gamma_{f_0(1710)\to KK} = 0.48 \pm 0.15 \quad [53], \tag{61}$$

$$\Gamma_{f_0(1710)\to\eta\eta}/\Gamma_{f_0(1710)\to KK} = 0.46^{+0.70}_{-0.38} \quad [54], \tag{62}$$

$$\Gamma_{f_0(1710)\to\eta\eta}/\Gamma_{f_0(1710)\to\pi\pi} = 2.40 \pm 1.04 \quad [51, 53]. \tag{63}$$

In all cases, the $f_0(1500)$ data are off by several standard deviations from our theoretical results, while there is good agreement with the results for $f_0(1710)$. We have also considered decays involving the η' meson. Since the threshold for $\eta\eta'$ decays is at approximately 1.5 GeV, it suffices to consider decays of f_0^H only. The value $\lambda_1 = -4.1 \mp 0.7$ yields

$$\Gamma_{f_0^H\to\eta\eta'} = 12.7^{+1.1}_{-1.4}\ \text{MeV}, \tag{64}$$

$$\Gamma_{f_0^H\to\eta\eta'}/\Gamma_{f_0^H\to\pi\pi} = 0.26^{-0.03}_{+0.04}, \tag{65}$$

$$\Gamma_{f_0^H\to\eta\eta'}/\Gamma_{f_0^H\to\eta\eta} = 0.26^{+0.04}_{-0.05}, \tag{66}$$

$$\Gamma_{f_0^H\to\eta\eta'}/\Gamma_{f_0^H\to KK} = 0.05 \pm 0.01, \tag{67}$$

whereas experimental data read

$$\Gamma_{f_0(1500)\to\eta\eta'} = (2.1 \pm 1.0)\ \text{MeV}, \tag{68}$$

$$\Gamma_{f_0(1500)\to\eta\eta'}/\Gamma_{f_0(1500)\to\pi\pi} = 0.055 \pm 0.024, \tag{69}$$

$$\Gamma_{f_0(1500)\to\eta\eta'}/\Gamma_{f_0(1500)\to\eta\eta} = 0.38 \pm 0.16. \tag{70}$$

The decay ratio $\Gamma_{f_0(1500)\to\eta\eta'}/\Gamma_{f_0(1500)\to KK}$ is unknown; there are also no data for the $\eta\eta'$ decay channel of $f_0(1710)$. Still we observe that neither $\Gamma_{f_0^H\to\eta\eta'}$ nor $\Gamma_{f_0^H\to\eta\eta'}/\Gamma_{f_0^H\to\pi\pi}$ describe the corresponding experimental results for $f_0(1500)$. Indeed the only piece of experimental data regarding $f_0(1500)$ that is described by our fit results is the one for the $\eta\eta'/\eta\eta$ decay ratio. Nonetheless, all the other results regarding decay ratios obtained by our analysis clearly demonstrate the correspondence of our predominantly strange state f_0^H to $f_0(1710)$; f_0^L was found to correspond to $f_0(1370)$ already in the discussion of the $\pi\pi$ decay channel. Consequently, we conclude that $f_0(1370)$ and $f_0(1710)$ are favored as scalar $\bar{q}q$ states. However, we also stress again that the mass of our f_0^H remains too low when compared to $m_{f_0(1710)}$ due to a missing scalar-glueball state expected to shift $m_{f_0^H}$ to $m_{f_0(1710)}$ by level repulsion.

2. Mixing in the pseudoscalar-isoscalar sector

Our Lagrangian (2) implements the mixing of two pure pseudoscalar isosinglet states, $\eta_N \equiv (\bar{u}u + \bar{d}d)/\sqrt{2}$ and $\eta_S \equiv \bar{s}s$. The mixing term is presented in Eq. (19). The mass terms for η_N (17) and η_S (18) are determined by our fit parameters presented in Table III. The same parameters also determine the η-η' mixing angle as [see Eqs. (A12)–(A16)]

$$\theta_\eta = -44.6°. \tag{71}$$

The result is close to maximal mixing; i.e., our result suggests a slightly larger mixing than those of Ref. [55].

3. The axial-vector kaon state K_1

The K_1 state has not been assigned to a physical resonance and included into our fit, because the PDG listing suggests two distinct assignment candidates, $K_1(1270)$ and $K_1(1400)$, expected to mix [39]. Therefore, mass and decay widths are left as predictions of this work.

There are three decay widths of the K_1 state that can be calculated within our model at tree level: $K_1 \to K^\star\pi$, ρK, and ωK. They account for approximately 70% of the full $K_1(1270)$ decay width and almost 100% of the full $K_1(1400)$ decay width [1]. Using the parameter values stated in Table III it is possible to calculate the mass, Eq. (32), as well as the decay width [via the generic decay-width formula (B46)] of our K_1 state. We obtain the following results:

$$\begin{aligned} m_{K_1} &= 1282\ \text{MeV}, & \Gamma_{K_1\to K^\star\pi} &= 205\ \text{MeV}, \\ \Gamma_{K_1\to\rho K} &= 44\ \text{MeV}, & \Gamma_{K_1\to\omega K} &= 15\ \text{MeV}. \end{aligned} \tag{72}$$

The mass is within 2σ of $m_{K_1(1270)} = (1272 \pm 7)$ MeV and thus rather close to the experimental result. However, the value of the full decay width is 264 MeV, while the PDG data read $\Gamma_{K_1(1270)} = (90 \pm 20)$ MeV and $\Gamma_{K_1(1400)} = (174 \pm 13)$ MeV. Our result is therefore approximately three times too large when compared to the data for $K_1(1270)$ and approximately 50% too large when compared to the data for $K_1(1400)$; errors have been omitted from the calculation. These results demonstrate the necessity to include a pseudovector $I(J^{\text{PC}}) = 1(1^{+-})$ nonet into our model and implement its mixing with the already present axial-vector nonet. A possible mixing term between an axial-vector nonet A_1 and a pseudovector nonet B_1 reads

$$\text{Tr}\,(\Delta[A_1^\mu, B_{1\mu}]), \tag{73}$$

with Δ from Eq. (8). Various studies have indeed found the mixing to be non-negligible [39]; see also Ref. [56].

4. Branching ratios of $a_0(1450)$

As a consequence of our fit we can determine the branching ratio of the resonance $a_0(1450)$ into KK, $\pi\eta$,

and $\pi\eta'$. We obtain the following values [see Eqs. (B1), (B2), and (B11)]:

$$\begin{aligned}\Gamma_{a_0\to\eta\pi} &= (115.4 \pm 6.2)\ \text{MeV},\\ \Gamma_{a_0\to\eta'\pi} &= (21.5 \pm 1.4)\ \text{MeV},\\ \Gamma_{a_0\to KK} &= (128.8 \pm 3.9)\ \text{MeV}.\end{aligned} \tag{74}$$

This leads to the following branching ratios:

$$\frac{\Gamma_{a_0\to\eta'\pi}}{\Gamma_{a_0\to\eta\pi}} = 0.19 \pm 0.02, \qquad \frac{\Gamma_{a_0\to KK}}{\Gamma_{a_0\to\eta\pi}} = 1.12 \pm 0.07, \tag{75}$$

which should be compared with the experimental results [1]

$$\begin{aligned}\frac{\Gamma_{a_0(1450)\to\eta'\pi}}{\Gamma_{a_0(1450)\to\eta\pi}} &= 0.35 \pm 0.16,\\ \frac{\Gamma_{a_0(1450)\to KK}}{\Gamma_{a_0(1450)\to\eta\pi}} &= 0.88 \pm 0.23.\end{aligned} \tag{76}$$

Our results are, within errors, consistent with the data.

5. Contributions to the mass of the ρ meson

The mass of the ρ meson consists of three terms,

$$m_\rho^2 = m_1^2 + \frac{1}{2}(h_1 + h_2 + h_3)\phi_N^2 + \frac{h_1}{2}\phi_S^2. \tag{77}$$

The first term m_1^2 is generated by the condensation of the dilaton field G, $m_1^2 \propto G_0^2$. The second term is proportional to the chiral condensate ϕ_N^2. In the large-N_c limit the parameter $h_1 = 0$ and we can determine the terms from the results of the fit: $m_1 = 0.643$ GeV and $\sqrt{(h_2 + h_3)/2}\phi_N = 0.447$ GeV. It turns out that the glueball-driven term is dominant.

It is interesting to note that models based on QCD sum rules [57] or Brown-Rho scaling [58] predict that $m_\rho^k \propto \phi_N$, where $k = 2$ in the first and $k = 3$ in the latter case. The order parameter for chiral symmetry breaking ϕ_N decreases as a function of nuclear matter density n: for small densities it is well known (see, e.g., Ref. [57]) that

$$\frac{\phi_N|_n}{\phi_N|_{\text{vacuum}}} \approx 1 - 0.3\frac{n}{n_0},$$

so these models predict a substantial decrease of m_ρ already at nuclear matter saturation density, n_0. In this respect, it is interesting to evaluate the value of the ρ mass at n_0 according to Eq. (77). We assume that the glueball-driven term m_1^2 does not vary. This can be motivated by considering that the glueball is massive and a substantial decrease in its mass may occur only at much higher density. Assuming that the linear dependence on the density of the condensate holds up to saturation density, we obtain that m_ρ decreases by about 70 MeV compared to 90–130 MeV predicted by Refs. [57,58].

Obviously, these considerations are only qualitative but could represent the starting point of interesting studies of vector mesons in the medium, which is an important aim of several experimental investigations [59]. To this end, one has to calculate the behavior of the dilaton and chiral condensates in the medium within the same theoretical framework.

IV. CONCLUSIONS

We have presented a linear sigma model with three quark flavors. The model implements the symmetries of QCD, the discrete CPT symmetry, the global chiral $U(N_f)_L \times U(N_f)_R$ symmetry, and the breaking mechanisms of the last: spontaneous (due to the chiral condensate), explicit (due to nonvanishing quark masses), as well as at the quantum level [the $U(1)_A$ anomaly]. Moreover, it implements also dilatation symmetry and its breaking (the so-called trace anomaly) in the YM sector of the theory. In this way, besides explicit breaking of dilatation symmetries arising from the nonzero current quark masses and the trace and axial anomalies in the gauge sector, all other interaction terms in our Lagrangian carry mass dimension equal to four. Furthermore, requiring analyticity in the fields makes the number of allowed terms finite.

The model has been used to describe meson states up to energies of $\sim$1.7 GeV. This energy region exhibits numerous resonances, related by scattering reactions and decays. For this reason, a realistic model of QCD degrees of freedom in the mentioned energy region should describe as many of the resonances as possible. Thus, we have constructed a linear sigma model that contains scalar (two isoscalars, f_0^L and f_0^H, as well as an isotriplet, a_0, and two isodoublets, $K_0^\star$), pseudoscalar (π, K, η, η'), vector (ρ, ω, $K^\star$, ϕ), and axial-vector [a_1, K_1, $f_1(1285)$, $f_1(1420)$] degrees of freedom. We have thus constructed a single model that contains (pseudo)scalars and (axial-) vectors both in the nonstrange and strange channels. To our knowledge, this is the first time that such a comprehensive approach has been presented.

The model, dubbed extended linear sigma model, has allowed us to study the overall phenomenology of mesons and, in particular, to explore the nature of scalar and axial-vector resonances. In order to test our model we have performed a global fit to 21 experimental quantities involving both the (pseudo)scalar and the (axial-)vector masses and decays. Due to mixing with the scalar glueball (not included here explicitly, because its coupling to the other mesons was neglected), we did not include the scalar-isoscalar resonances in the fit. Similarly, we have omitted the axial-vector resonance K_1, due to the fact that in reality a large mixing of two kaonic fields from the 1^{++} and 1^{+-} nonets takes place.

One of the central questions of our discussion has been the assignment of the scalar states: to this end we have tested the possible scenarios for the isotriplet and

isodoublet scalar states by assigning our scalar fields a_0 to $a_0(980)$ or $a_0(1450)$ and $K_0^\star$ to $K_0^\star(800)$ or $K_0^\star(1430)$. The outcome is univocal: the global fit works well only if the states $a_0(1450)$ and $K_0^\star(1430)$ are interpreted as quark-antiquark states. On the contrary, the other combinations deliver unacceptably large values of χ^2 (see Table I). We thus conclude that the scalar $I = 1$ and $I = 1/2$ states lie above 1 GeV and have to be identified with the resonances $a_0(1450)$ and $K_0^\star(1430)$. Moreover, the overall phenomenology described by the fit is very good (see Table II). It is then possible to properly describe many different mesonic masses and decays within a unified treatment based on the symmetries of QCD. It should be stressed that the inclusion of the (axial-)vector mesons has a crucial impact on our results and represents the most important new ingredient of our approach. The good agreement with data also shows that the axial-vector mesons can be interpreted, just as their vector chiral partners, as quark-antiquark states.

We have then studied the consequences of our fit. We have primarily concentrated on the scalar-isoscalar sector which was not included in the fit. In the limit $N_c \to \infty$ it is possible to make clear predictions for the two states f_0^L and f_0^H. Their masses lie above 1 GeV and their decay patterns have led us to identify f_0^L with (predominantly) $f_0(1370)$ and f_0^H with (predominantly) $f_0(1710)$. The theoretical decay rates of f_0^L are in agreement with experiment; f_0^H decays only into kaons, but turns out to be too wide. At a qualitative level, this large-N_c result clearly shows that also the scalar-isoscalar quark-antiquark states lie above 1 GeV. The overall situation in the scalar-isoscalar sector can be slightly improved when adding large-N_c suppressed terms. Some of these terms correspond to interactions between mesons and a glueball state. These were neglected here, but are necessary for a full quantitative study. Then starting from $\sigma_N = \sqrt{1/2}(\bar{u}u + \bar{d}d)$, $G = gg$, and $\sigma_S = \bar{s}s$ one aims to describe properly $f_0(1370)$, $f_0(1500)$, and $f_0(1710)$.

Additionally, we have studied other consequences of the fit, such as predictions for the $\eta\eta$ channel of scalar-isoscalar states, the η-η' mixing, the prediction for the axial-vector kaonic state, and for the a_0 branching ratios. Finally, we have also discussed the origin of the mass of the ρ meson and, at a qualitative level, its possible value at nuclear matter density.

There is, however, one question that remains open. Interpreting resonances above 1 GeV as $\bar{q}q$ states leads to questions about the nature of $f_0(500)$, $a_0(980)$, $f_0(980)$, and $K_0^\star(800)$. Their presence is necessary for the correct description of $\pi\pi$ scattering lengths (see, e.g., Ref. [15]). There are two possibilities: they can arise (i) as (quasi) molecular states of $\pi\pi$ or KK, respectively, or (ii) as tetraquark states [43,60]. The question is whether the attraction is large enough so that these states are bound, or the attraction is not sufficient so that they are (unstable) resonances in the continuum. This question and deciding whether possibility (i) or (ii) is realized in nature represent interesting starting points for future studies, along the lines of the Bethe-Salpeter approach of Ref. [61], the lattice approach of Ref. [62], or even holographic approaches such as those presented in Ref. [63]. In either case, one may include the low-lying isoscalar states as interpolating fields in our Lagrangian, such as has been done in Ref. [42].

The present model can be also studied in the baryonic sector (see Ref. [16] for the two-flavor case). The very same ideas of chiral symmetry and dilatation invariance can be applied to the baryonic sector as well. The extension of the model to three flavors in the baryonic sector would surely represent an interesting problem: a multitude of data on decays and masses is available to make a precise test of our approach.

Additionally, restoration of chiral symmetry at nonzero temperature and density is one of the fundamental questions of modern hadron physics; see, e.g., Refs. [10,64], in which the two-flavor version of this model has been studied at nonzero density, or Ref. [65] for alternative approaches to the exploration of nonzero chemical potential. Linear sigma models are appropriate to study chiral symmetry restoration because they contain from the onset not only (pseudo)scalar and (axial-)vector mesons but also their chiral partners; mass degeneration of chiral partners represents a signal for the chiral transition. Therefore, we also plan to apply the model to study chiral symmetry restoration at nonzero temperatures and densities.

ACKNOWLEDGMENTS

Gy. Wolf and P. Kovács thank the Institute for Theoretical Physics of Goethe University for its hospitality, where part of this work was done. They were partially supported by the Hungarian OTKA funds T71989 and T101438. The work of D. Parganlija and F. Giacosa was supported by the Foundation of the Polytechnical Society Frankfurt. This work was financially supported by the Helmholtz International Center for FAIR within the framework of the LOEWE program (Landesoffensive zur Entwicklung Wissenschaftlich-Ökonomischer Exzellenz) launched by the State of Hesse. D. H. Rischke thanks R. Longacre and R. Pisarski for enlightening discussions.

APPENDIX A: TREE-LEVEL MASSES

After spontaneous symmetry breaking (see Sec. II B), from the quadratic terms of the Lagrangian the (squared) mass matrices for the different fields are read off as

$$(m_S^2)_{ij} = S_{ip}(m_0^2\delta_{pq} + 4F_{pqlm}\phi_l\phi_m)S_{qj}, \tag{A1}$$

$$(m_P^2)_{ij} = S_{ip}(m_0^2\delta_{pq} - 9c_1G_{plm}\phi_l\phi_mG_{ql'm'}\phi_{l'}\phi_{m'} + 4H_{pq,lm}\phi_l\phi_m)S_{qj}, \tag{A2}$$

$$(m_V^2)_{ij} = S_{ip}(m_1^2\delta_{pq} + J_{pqlm}\phi_l\phi_m)S_{qj}, \tag{A3}$$

$$(m_A^2)_{ij} = S_{ip}(m_1^2\delta_{pq} + J'_{pqlm}\phi_l\phi_m)S_{qj}, \tag{A4}$$

where S_{qj} is the (9×9) transformation matrix to the nonstrange-strange base,

$$S = \frac{1}{\sqrt{3}}\begin{pmatrix} \sqrt{2} & 0 & \dots & 1 \\ 0 & 1 & \dots & 0 \\ \vdots & \vdots & \ddots & \vdots \\ 1 & 0 & \dots & -\sqrt{2} \end{pmatrix}, \tag{A5}$$

and the F, H, G, J, J' coefficient tensors are

$$F_{ijkl} = \frac{\lambda_1}{4}(\delta_{ij}\delta_{kl} + \delta_{ik}\delta_{jl} + \delta_{il}\delta_{jk}) + \frac{\lambda_2}{8}(d_{ijm}d_{klm} + d_{ikm}d_{jlm} + d_{ilm}d_{jkm}), \tag{A6}$$

$$H_{ij,kl} = \frac{\lambda_1}{4}\delta_{ij}\delta_{kl} + \frac{\lambda_2}{8}(d_{ijm}d_{klm} + f_{ikm}f_{jlm} + f_{ilm}f_{jkm}), \tag{A7}$$

$$G_{ijk} = \frac{1}{6}\Big[d_{ijk} + \frac{9}{2}d_{000}\delta_{i0}\delta_{j0}\delta_{k0} - \frac{3}{2}(\delta_{i0}d_{jk0} + \delta_{j0}d_{ik0} + \delta_{k0}d_{ij0})\Big], \tag{A8}$$

$$J_{ijkl} = g_1^2 f_{ikm}f_{jlm} + \frac{h_1}{2}\delta_{ij}\delta_{kl} + \frac{h_2}{2}d_{ijm}d_{klm} + \frac{h_3}{4}\times(d_{ikm}d_{jlm} + d_{ilm}d_{jkm} - f_{ikm}f_{jlm} - f_{ilm}f_{jkm}), \tag{A9}$$

$$J'_{ijkl} = g_1^2 d_{ikm}d_{jlm} + \frac{h_1}{2}\delta_{ij}\delta_{kl} + \frac{h_2}{2}d_{ijm}d_{klm} - \frac{h_3}{4}\times(d_{ikm}d_{jlm} + d_{ilm}d_{jkm} - f_{ikm}f_{jlm} - f_{ilm}f_{jkm}). \tag{A10}$$

As can be seen from Eqs. (17)–(19) and (22)–(24), there is a mixing in the pseudoscalar and scalar N-S sectors, which can be resolved by the following two-dimensional orthogonal transformations

$$O_{\eta/\sigma} = \begin{pmatrix} \cos\theta_{\eta/\sigma} & \sin\theta_{\eta/\sigma} \\ -\sin\theta_{\eta/\sigma} & \cos\theta_{\eta/\sigma} \end{pmatrix}, \tag{A11}$$

where $\theta_{\eta/\sigma}$ are the pseudoscalar and scalar mixing angles. The (squared) mass eigenvalues can be written with the help of the mixing angles as

$$\begin{aligned} m^2_{\eta_1/\sigma_1} &= m^2_{\eta_N/\sigma_N}\cos^2\theta_{\eta/\sigma} + m^2_{\eta_{NS}/\sigma_{NS}}\sin 2\theta_{\eta/\sigma} \\ &\quad + m^2_{\eta_S/\sigma_S}\sin^2\theta_{\eta/\sigma}, \\ m^2_{\eta_2/\sigma_2} &= m^2_{\eta_N/\sigma_N}\sin^2\theta_{\eta/\sigma} - m^2_{\eta_{NS}/\sigma_{NS}}\sin 2\theta_{\eta/\sigma} \\ &\quad + m^2_{\eta_S/\sigma_S}\cos^2\theta_{\eta/\sigma}, \end{aligned} \tag{A12}$$

where, if we require that $m^2_{\eta_2/\sigma_2} > m^2_{\eta_1/\sigma_1}$, the mixing angles are given by

$$\sin\theta_{\eta/\sigma} = -\mathrm{sign}(m^2_{\eta_{NS}/\sigma_{NS}})\frac{1}{\sqrt{2}} \times\sqrt{1 - \frac{m^2_{\eta_S/\sigma_S} - m^2_{\eta_N/\sigma_N}}{\sqrt{(m^2_{\eta_N/\sigma_N} - m^2_{\eta_S/\sigma_S})^2 + 4m^4_{\eta_{NS}/\sigma_{NS}}}}}, \tag{A13}$$

$$\cos\theta_{\eta/\sigma} = \frac{1}{\sqrt{2}}\sqrt{1 + \frac{m^2_{\eta_S/\sigma_S} - m^2_{\eta_N/\sigma_N}}{\sqrt{(m^2_{\eta_N/\sigma_N} - m^2_{\eta_S/\sigma_S})^2 + 4m^4_{\eta_{NS}/\sigma_{NS}}}}}. \tag{A14}$$

It can be seen that if $m^2_{\eta_{NS}/\sigma_{NS}} > 0$, then $-\pi/2 < \theta_{\eta/\sigma} < 0$, and if $m^2_{\eta_{NS}/\sigma_{NS}} < 0$, then $0 < \theta_{\eta/\sigma} < \pi/2$. Substituting these expressions into Eq. (A12) it is found that

$$m^2_{\eta_1/\sigma_1} = \frac{1}{2}\Big[m^2_{\eta_N/\sigma_N} + m^2_{\eta_S/\sigma_S} - \sqrt{(m^2_{\eta_N/\sigma_N} - m^2_{\eta_S/\sigma_S})^2 + 4m^4_{\eta_{NS}/\sigma_{NS}}}\Big], \tag{A15}$$

$$m^2_{\eta_2/\sigma_2} = \frac{1}{2}\Big[m^2_{\eta_N/\sigma_N} + m^2_{\eta_S/\sigma_S} + \sqrt{(m^2_{\eta_N/\sigma_N} - m^2_{\eta_S/\sigma_S})^2 + 4m^4_{\eta_{NS}/\sigma_{NS}}}\Big], \tag{A16}$$

from which it is obvious that the condition $m^2_{\eta_2/\sigma_2} > m^2_{\eta_1/\sigma_1}$ is fulfilled. In this way we know that m_{η_2} must be identified as $m_{\eta'}$, and similarly for σ.

APPENDIX B: DECAY WIDTHS

In this section we show the explicit form of some of the most relevant decay widths calculated from our model at tree level using Eq. (38). The formulas below are organized according to the type of the decaying particle.

1. Scalar-meson decay widths

At first we are considering the decays of the scalar isotriplet a_0, scalar kaon $K_0^\star$, and scalar isosinglets $f_0^{H/L}$. The a_0 state has three relevant decay channels, namely into $\eta\pi$, $\eta'\pi$, and KK, the first two of which are strongly connected due to the mixing between η and η'. The $a_0 \to \eta\pi$ and $a_0 \to \eta'\pi$ decay widths,[3] considering that in both cases $\mathcal{I} = 1$, read

[3]Obviously, the neutral and the charged a_0's have the same formulas for the decay widths.

$$\Gamma_{a_0\to\eta\pi}=\frac{1}{8m_{a_0}\pi}\times\left[\frac{(m_{a_0}^2-m_\eta^2-m_\pi^2)^2-4m_\eta^2m_\pi^2}{4m_{a_0}^4}\right]^{1/2}|\mathcal{M}_{a_0\to\eta\pi}|^2, \tag{B1}$$

$$\Gamma_{a_0\to\eta'\pi}=\frac{1}{8m_{a_0}\pi}\left[\frac{(m_{a_0}^2-m_{\eta'}^2-m_\pi^2)^2-4m_{\eta'}^2m_\pi^2}{4m_{a_0}^4}\right]^{1/2}\times|\mathcal{M}_{a_0\to\eta'\pi}|^2, \tag{B2}$$

with the following transition matrix elements,

$$\mathcal{M}_{a_0\to\eta\pi}=\cos\theta_\pi\mathcal{M}_{a_0\to\eta_N\pi}(m_\eta)+\sin\theta_\pi\mathcal{M}_{a_0\to\eta_S\pi}(m_\eta), \tag{B3}$$

$$\mathcal{M}_{a_0\to\eta'\pi}=\cos\theta_\pi\mathcal{M}_{a_0\to\eta_S\pi}(m_{\eta'})-\sin\theta_\pi\mathcal{M}_{a_0\to\eta_N\pi}(m_{\eta'}), \tag{B4}$$

where

$$\mathcal{M}_{a_0\to\eta_N\pi}(m)=A_{a_0\eta_N\pi}-B_{a_0\eta_N\pi}\frac{m_{a_0}^2-m^2-m_\pi^2}{2}+C_{a_0\eta_N\pi}m_{a_0}^2, \tag{B5}$$

$$\mathcal{M}_{a_0\to\eta_S\pi}(m)=A_{a_0\eta_S\pi}, \tag{B6}$$

and

$$A_{a_0\eta_N\pi}=Z_\pi^2(c_1\phi_S^2-\lambda_2)\phi_N, \tag{B7}$$

$$B_{a_0\eta_N\pi}=-2\frac{g_1^2\phi_N}{m_{a_1}^2}\left[1-\frac{1}{2}\frac{Z_\pi^2\phi_N^2}{m_{a_1}^2}(h_2-h_3)\right], \tag{B8}$$

$$C_{a_0\eta_N\pi}=g_1Z_\pi^2w_{a_1}, \tag{B9}$$

$$A_{a_0\eta_S\pi}=\frac{1}{2}c_1Z_\pi Z_{\eta_S}\phi_N^2\phi_S. \tag{B10}$$

The $a_0\to KK$ decay width includes two subchannels, $K^0\bar{K}^0$ and K^-K^+, which results in the isospin factor $\mathcal{I}=2$, and accordingly the decay width is found to be

$$\Gamma_{a_0\to KK}=\frac{1}{8m_{a_0}\pi}\sqrt{1-\left(\frac{2m_K}{m_{a_0}}\right)^2}\left|A_{a_0KK}-\frac{1}{2}B_{a_0KK}(m_{a_0}^2-2m_K^2)+C_{a_0KK}m_{a_0}^2\right|^2, \tag{B11}$$

where

$$A_{a_0KK}=\lambda_2Z_K^2\left(\phi_N-\frac{\phi_S}{\sqrt{2}}\right), \tag{B12}$$

$$B_{a_0KK}=Z_K^2w_{K_1}\left\{g_1-\frac{1}{2}w_{K_1}((g_1^2+h_2)\phi_N+\sqrt{2}(g_1^2-h_3)\phi_S)\right\}, \tag{B13}$$

$$C_{a_0KK}=-\frac{g_1}{2}Z_K^2w_{K_1}. \tag{B14}$$

Now turning to the scalar kaon there is only one relevant decay channel, $K_0^\star(\text{or}\,K_0)\to K\pi$, for which the decay width reads

$$\Gamma_{K_0\to K\pi}=\frac{3}{8\pi m_{K_0}}\left[\frac{(m_{K_0}^2-m_\pi^2-m_K^2)^2-4m_\pi^2m_K^2}{4m_{K_0}^4}\right]^{1/2}\times\left[A_{K_0K\pi}+(C_{K_0K\pi}+D_{K_0K\pi}-B_{K_0K\pi})\times\frac{m_{K_0}^2-m_K^2-m_\pi^2}{2}+C_{K_0K\pi}m_K^2+D_{K_0K\pi}m_\pi^2\right], \tag{B15}$$

where

$$A_{K_0K\pi}=\frac{Z_\pi Z_K Z_{K_0}}{\sqrt{2}}\lambda_2\phi_S, \tag{B16}$$

$$B_{K_0K\pi}=\frac{Z_\pi Z_K Z_{K_0}}{4}w_{a_1}w_{K_1}\left[2g_1\frac{w_{a_1}+w_{K_1}}{w_{a_1}w_{K_1}}+(2h_3-h_2-3g_1^2)\phi_N-\sqrt{2}(g_1^2+h_2)\phi_S\right], \tag{B17}$$

$$C_{K_0K\pi}=\frac{Z_\pi Z_K Z_{K_0}}{2}[-g_1(iw_{K^\star}+w_{K_1})+\sqrt{2}iw_{K^\star}w_{K_1}(g_1^2-h_3)\phi_S], \tag{B18}$$

$$D_{K_0K\pi}=\frac{Z_\pi Z_K Z_{K_0}}{4}\{2g_1(iw_{K^\star}-w_{a_1})+iw_{K^\star}w_{a_1}[(2h_3-h_2-3g_1^2)\phi_N+\sqrt{2}(g_1^2+h_2)\phi_S]\}. \tag{B19}$$

Finally, for the $f_0^{L/H}$ particles there are two relevant decay channels: the two-pion and the two-kaon channels. It is important to note that due to the particle mixing between f_0^L and f_0^H the matrix elements are linear combinations that depend on the scalar mixing angle θ_σ (see Appendix A), as can be seen explicitly below. The decay widths in the $\pi\pi$ channel are

$$\Gamma_{f_0^L\to\pi\pi}=\frac{3}{32\pi m_{f_0^L}}\sqrt{1-\left(\frac{2m_\pi}{m_{f_0^L}}\right)^2}|\mathcal{M}_{f_0^L\to\pi\pi}|^2, \tag{B20}$$

$$\Gamma_{f_0^H\to\pi\pi}=\frac{3}{32\pi m_{f_0^H}}\sqrt{1-\left(\frac{2m_\pi}{m_{f_0^H}}\right)^2}|\mathcal{M}_{f_0^H\to\pi\pi}|^2, \quad \text{(B21)}$$

where an isospin factor of $3/2$ was considered[4] and the matrix elements are

$$\mathcal{M}_{f_0^L\to\pi\pi}=-\sin\theta_\sigma\mathcal{M}^H_{f_0\pi}(m_{f_0^L})+\cos\theta_\sigma\mathcal{M}^L_{f_0\pi}(m_{f_0^L}), \quad \text{(B22)}$$

$$\mathcal{M}_{f_0^H\to\pi\pi}=\cos\theta_\sigma\mathcal{M}^H_{f_0\pi}(m_{f_0^H})+\sin\theta_\sigma\mathcal{M}^L_{f_0\pi}(m_{f_0^H}), \quad \text{(B23)}$$

$$\mathcal{M}^L_{f_0\pi}(m)=2Z_\pi^2\phi_N\left\{\frac{g_1^2}{2}\frac{m^2}{m_{a_1}^2}\left[1+\left(1-\frac{2m_\pi^2}{m^2}\right)\times\frac{m_1^2+h_1\phi_S^2/2+2\delta_N}{m_{a_1}^2}\right]-\left(\lambda_1+\frac{\lambda_2}{2}\right)\right\}, \quad \text{(B24)}$$

$$\mathcal{M}^H_{f_0\pi}(m)=2Z_\pi^2\phi_S\left\{-\frac{g_1^2}{4}\frac{m^2}{m_{a_1}^2}\left(1-\frac{2m_\pi^2}{m^2}\right)\frac{h_1\phi_N^2}{m_{a_1}^2}-\lambda_1\right\}. \quad \text{(B25)}$$

In the KK channel, where $I=2$, the decay widths read

$$\Gamma_{f_0^H\to KK}=\frac{1}{8\pi m_{f_0^H}}\sqrt{1-\left(\frac{2m_K}{m_{f_0^H}}\right)^2}|\mathcal{M}_{f_0^H\to KK}|^2, \quad \text{(B26)}$$

$$\Gamma_{f_0^L\to KK}=\frac{1}{8\pi m_{f_0^L}}\sqrt{1-\left(\frac{2m_K}{m_{f_0^L}}\right)^2}|\mathcal{M}_{f_0^L\to KK}|^2, \quad \text{(B27)}$$

where the matrix elements, using the notations $H_N\equiv(g_1^2+2h_1+h_2)/4$ and $H_S\equiv(g_1^2+h_1+h_2)/2$, are

$$\mathcal{M}_{f_0^L\to KK}=-\sin\theta_\sigma\mathcal{M}^H_{f_0K}(m_{f_0^L})+\cos\theta_\sigma\mathcal{M}^L_{f_0K}(m_{f_0^L}), \quad \text{(B28)}$$

$$\mathcal{M}_{f_0^H\to KK}=\cos\theta_\sigma\mathcal{M}^H_{f_0K}(m_{f_0^H})+\sin\theta_\sigma\mathcal{M}^L_{f_0K}(m_{f_0^H}), \quad \text{(B29)}$$

$$\mathcal{M}^L_{f_0K}(m)=-Z_K^2\Big[(2\lambda_1+\lambda_2)\phi_N-\frac{\lambda_2}{\sqrt{2}}\phi_S+g_1w_{K_1}(m_K^2-m^2)+w_{K_1}^2\Big(2H_N\phi_N-\frac{h_3-g_1^2}{\sqrt{2}}\phi_S\Big)\times\frac{m^2-2m_K^2}{2}\Big], \quad \text{(B30)}$$

$$\mathcal{M}^H_{f_0K}(m)=-Z_K^2\Big[2(\lambda_1+\lambda_2)\phi_S-\frac{\lambda_2}{\sqrt{2}}\phi_N+\sqrt{2}g_1w_{K_1}(m_K^2-m^2)+w_{K_1}^2\Big(2H_S\phi_S-\frac{h_3-g_1^2}{\sqrt{2}}\phi_N\Big)\frac{m^2-2m_K^2}{2}\Big]. \quad \text{(B31)}$$

2. Vector-meson decay widths

In the case of the vector mesons we are considering the decays of the ρ meson, the $K^\star$ vector kaon, and the ϕ meson. All these particles have only one relevant decay channel. The first is the $\rho\to\pi\pi$ decay which has the following quite simple decay-width formula:

$$\Gamma_{\rho\to\pi\pi}=\frac{m_\rho^5}{48\pi m_{a_1}^4}\left[1-\left(\frac{2m_\pi}{m_\rho}\right)^2\right]^{3/2}\left[g_1Z_\pi^2-\frac{g_2}{2}(Z_\pi^2-1)\right]^2. \quad \text{(B32)}$$

The next one is the $K^\star\to K\pi$ decay, in case of which the decay width reads

$$\Gamma_{K^\star\to K\pi}=\frac{m_{K^\star}}{8\pi}\left[\frac{(m_{K^\star}^2-m_\pi^2-m_K^2)^2-4m_\pi^2m_K^2}{4m_{K^\star}^4}\right]^{3/2}\times(A_{K^\star K\pi}-B_{K^\star K\pi}+C_{K^\star K\pi})^2, \quad \text{(B33)}$$

where the constants are defined as

$$\begin{aligned}A_{K^\star K\pi}&=\frac{1}{2}Z_\pi Z_K[-g_1+\sqrt{2}w_{K_1}(g_1^2-h_3)\phi_S],\\ B_{K^\star K\pi}&=\frac{1}{4}Z_\pi Z_K[2g_1+w_{a_1}(-3g_1^2-h_2+2h_3)\phi_N+\sqrt{2}w_{a_1}(g_1^2+h_2)\phi_S],\\ C_{K^\star K\pi}&=\frac{1}{2}Z_\pi Z_K w_{a_1}w_{K_1}g_2m_{K^\star}^2.\end{aligned} \quad \text{(B34)}$$

Finally, the $\phi\to KK$ decay width reads

$$\Gamma_{\phi\to KK}=\frac{m_\phi^5}{192\pi m_{K_1}^4}\left[1-\left(\frac{2m_K}{m_\phi}\right)^2\right]^{3/2}\times\left[2g_1Z_K^2\left(1+\frac{\delta_N-\delta_S}{m_\phi^2}\right)-g_2(Z_K^2-1)\right]^2. \quad \text{(B35)}$$

[4]There are two subchannels, namely the $\pi^+\pi^-$ and the $\pi^0\pi^0$, which would mean $I=2$. However, since the two π^0 are indistinguishable, the solid-angle integral (there is no angular dependence at tree level) ends up as 2π instead of 4π, which means a factor of $1/2$ in case of $\pi^0\pi^0$ compared to $\pi^+\pi^-$, thus $I=1/2+1$.

3. Axial-vector-meson decay widths

Turning to axial-vector mesons, the considered decays are the a_1 decay with two relevant channels and the f_{1S} decay with one relevant channel. Since, in case of the $a_1 \to \rho\pi$ and $f_{1S} \to KK^\star$ decays, the decaying as well as one of the resulting particles are (axial-)vector mesons, the matrix elements have a more complicated form than in the previous cases, as can be seen below. The first considered decay width is the one of the $a_1 \to \pi\gamma$ process, which takes the following simple form:

$$\Gamma_{a_1\to\pi\gamma} = \frac{e^2 g_1^2 \phi_N^2}{96\pi m_{a_1}} Z_\pi^2 \left[1 - \left(\frac{m_\pi}{m_{a_1}}\right)^2\right]^3. \tag{B36}$$

In case of the $a_1 \to \rho\pi$ decay width one has to consider two channels ($\rho^+\pi^-$, $\rho^-\pi^+$); thus $\mathcal{I} = 2$ and the decay width is found to be

$$\begin{aligned}\Gamma_{a_1\to\rho\pi} = {} & \frac{1}{12 m_{a_1}\pi}\left[\frac{(m_{a_1}^2 - m_\rho^2 - m_\pi^2)^2 - 4m_\rho^2 m_\pi^2}{4m_{a_1}^4}\right]^{1/2} \\ & \times\left[|V_{\mu\nu}|^2 - \frac{|V_{\mu\nu}k_\rho^\nu|^2}{m_\rho^2} - \frac{|V_{\mu\nu}k_{a_1}^\mu|^2}{m_{a_1}^2} + \frac{|V_{\mu\nu}k_{a_1}^\mu k_\rho^\nu|^2}{m_\rho^2 m_{a_1}^2}\right],\end{aligned} \tag{B37}$$

where $V_{\mu\nu}$ is the vertex following from the relevant part of the Lagrangian,

$$\begin{aligned}V_{\mu\nu} = {} & iZ_\pi\phi_N\Big\{(g_1^2 - h_3)g_{\mu\nu} \\ & + \frac{g_1 g_2}{m_{a_1}^2}[k_{\pi\mu}k_{a_1\nu} + k_{\rho\mu}k_{\pi\nu} - k_\pi\cdot(k_\rho + k_{a_1})g_{\mu\nu}]\Big\},\end{aligned} \tag{B38}$$

and $k_{a_1}^\mu = (m_{a_1}, \mathbf{0})$, $k_\rho^\mu = (E_\rho, \mathbf{k})$, and $k_\pi^\mu = (E_\pi, -\mathbf{k})$ are the four-momenta of a_1, ρ, and π in the rest frame of a_1, respectively. Using the following kinematic relations,

$$\begin{aligned}k_\pi\cdot k_\rho &= \frac{m_{a_1}^2 - m_\rho^2 - m_\pi^2}{2}, \\ k_{a_1}\cdot k_\pi &= m_{a_1}E_\pi = \frac{m_{a_1}^2 + m_\pi^2 - m_\rho^2}{2}, \\ k_{a_1}\cdot k_\rho &= m_{a_1}E_\rho = \frac{m_{a_1}^2 + m_\rho^2 - m_\pi^2}{2}, \\ \mathbf{k}^2 &= \frac{(m_{a_1}^2 - m_\pi^2 - m_\rho^2)^2 - 4m_\pi^2 m_\rho^2}{4m_{a_1}^2},\end{aligned} \tag{B39}$$

the terms in Eq. (B37) are given by

$$\begin{aligned}|V_{\mu\nu}|^2 &= Z_\pi^2\phi_N^2\left\{4(g_1^2 - h_3)^2 + \frac{g_1^2 g_2^2}{m_{a_1}^4}\left[\frac{5}{2}(m_{a_1}^2 - m_\rho^2)^2 + \frac{1}{2}m_\pi^2(2m_{a_1}^2 + 2m_\rho^2 - m_\pi^2)\right] - 6\frac{g_1 g_2(g_1^2 - h_3)}{m_{a_1}^2}(m_{a_1}^2 - m_\rho^2)\right\}, \\ \frac{|V_{\mu\nu}k_\rho^\nu|^2}{m_\rho^2} &= Z_\pi^2\phi_N^2\left\{(g_1^2 - h_3)^2 - \frac{g_1^2 g_2^2}{m_\rho^2}(E_\rho^2 - m_\rho^2) + 2\frac{g_1 g_2(g_1^2 - h_3)}{m_\rho^2}(E_\pi^2 - m_\pi^2)\right\}, \\ \frac{|V_{\mu\nu}k_{a_1}^\nu|^2}{m_{a_1}^2} &= Z_\pi^2\phi_N^2\left\{(g_1^2 - h_3)^2 - \frac{g_1^2 g_2^2}{m_{a_1}^4}m_\rho^2\mathbf{k}^2 - 2\frac{g_1 g_2(g_1^2 - h_3)}{m_{a_1}^2}(E_\rho^2 - m_\rho^2)\right\}, \\ \frac{|V_{\mu\nu}k_{a_1}^\mu k_\rho^\nu|^2}{m_\rho^2 m_{a_1}^2} &= Z_\pi^2\phi_N^2\frac{(g_1^2 - h_3)^2}{m_\rho^2}E_\rho^2.\end{aligned} \tag{B40}$$

Analogously to the previous case, the width of the $f_{1S} \to KK^\star$ decay which includes four subchannels ($K^0\bar{K}^{\star 0}$, $\bar{K}^0 K^{\star 0}$, $K^- K^{\star +}$, $K^+ K^{\star -}$), resulting in $\mathcal{I} = 4$, becomes

$$\Gamma_{f_{1S}\to KK^\star} = \frac{1}{6 m_{f_{1S}}\pi}\left[\frac{(m_{f_{1S}}^2 - m_{K^\star}^2 - m_\pi^2)^2 - 4m_{K^\star}^2 m_K^2}{4m_{f_{1S}}^4}\right]^{1/2}\left[|\tilde{V}_{\mu\nu}|^2 - \frac{|\tilde{V}_{\mu\nu}k_{K^\star}^\nu|^2}{m_{K^\star}^2} - \frac{|\tilde{V}_{\mu\nu}k_{f_{1S}}^\mu|^2}{m_{f_{1S}}^2} + \frac{|\tilde{V}_{\mu\nu}k_{f_{1S}}^\mu k_{K^\star}^\nu|^2}{m_{K^\star}^2 m_{f_{1S}}^2}\right], \tag{B41}$$

where $\tilde{V}_{\mu\nu}$ has the same Lorentz structure as Eq. (B38) and the only difference is in the constants in front of the different terms. More explicitly,

$$\tilde{V}_{\mu\nu} = iZ_K\{A_{fKK}g_{\mu\nu} + B_{fKK}[k_{K\mu}k_{f_{1S}\nu} + k_{K^\star\mu}k_{K\nu} - k_K\cdot(k_{K^\star} + k_{f_{1S}})g_{\mu\nu}]\}, \tag{B42}$$

$$A_{fKK} = \frac{1}{4}[g_1^2(\sqrt{2}\phi_N - 6\phi_S) + \sqrt{2}h_2(\phi_N - \sqrt{2}\phi_S) + 4h_3\phi_S], \tag{B43}$$

$$B_{fKK} = -\frac{1}{\sqrt{2}}g_2 w_{K_1}. \tag{B44}$$

The kinematic relations are the same as in Eq. (B39) with the substitutions $a_1 \to f_{1S}$, $\pi \to K$, $\rho \to K^\star$, while the expressions analogous to Eq. (B40) are

$$\begin{aligned}
|\tilde{V}_{\mu\nu}|^2 &= Z_K^2\left\{4A_{fKK}^2 + B_{fKK}^2\left[\frac{5}{2}(m_{f_{1S}}^2 - m_{K^\star}^2)^2 + \frac{1}{2}m_K^2(2m_{f_{1S}}^2 + 2m_{K^\star}^2 - m_K^2)\right] - 6A_{fKK}B_{fKK}(m_{f_{1S}}^2 - m_{K^\star}^2)\right\},\\
\frac{|\tilde{V}_{\mu\nu}k_{K^\star}^\nu|^2}{m_{K^\star}^2} &= Z_K^2\{A_{fKK}^2 - B_{fKK}^2(E_{K^\star}^2 - m_{K^\star}^2) + 2A_{fKK}B_{fKK}(E_K^2 - m_K^2)\},\\
\frac{|\tilde{V}_{\mu\nu}k_{f_{1S}}^\nu|^2}{m_{f_{1S}}^2} &= Z_K^2\{A_{fKK}^2 - B_{fKK}^2 m_{K^\star}^2\mathbf{k}^2 - 2A_{fKK}B_{fKK}(E_{K^\star}^2 - m_{K^\star}^2)\},\\
\frac{|\tilde{V}_{\mu\nu}k_{f_{1S}}^\mu k_{K^\star}^\nu|^2}{m_{K^\star}^2 m_{f_{1S}}^2} &= Z_K^2\frac{A_{fKK}^2}{m_{K^\star}^2}E_{K^\star}^2.
\end{aligned} \tag{B45}$$

Analogously, the width for a generic decay of the form $K_1 \to VP$, where V denotes a vector and P a pseudoscalar state, reads

$$\begin{aligned}
\Gamma_{K_1\to VP} = \mathcal{I}\frac{k(m_{K_1}, m_V, m_P)}{8\pi m_{K_1}^2}\frac{1}{3}\Bigg[&|\tilde{V}_{K_1VP}^{\mu\nu}|^2 - \frac{|\tilde{V}_{K_1VP}^{\mu\nu}p_{K_1\mu}|^2}{m_{K_1}^2}\\
&- \frac{|\tilde{V}_{K_1VP}^{\mu\nu}p_{V\nu}|^2}{m_V^2} + \frac{|\tilde{V}_{K_1VP}^{\mu\nu}p_{K_1\mu}p_{V\nu}|^2}{m_V^2 m_{K_1}^2}\Bigg],
\end{aligned} \tag{B46}$$

where $\mathcal{I} = 3$ for the $K_1 \to \rho K$ and $K_1 \to K^\star\pi$ decays and $\mathcal{I} = 1$ for the $K_1 \to \omega_N K$ decay,

$$\begin{aligned}
k(m_a, m_b, m_c) = &\frac{1}{2m_a}\sqrt{m_a^4 - 2m_a^2(m_b^2 + m_c^2) + (m_b^2 - m_c^2)^2}\\
&\times\theta(m_a - m_b - m_c)
\end{aligned} \tag{B47}$$

(the theta function ensures that the decay width vanishes below threshold), and

$$\begin{aligned}
\tilde{V}_{K_1VP}^{\mu\nu} = i\{&A_{K_1}g^{\mu\nu} + B_{K_1}[p_V^\mu p_P^\nu + p_P^\mu p_{K_1}^\nu - (p_P\cdot p_V)g^{\mu\nu}\\
&- (p_{K_1}\cdot p_P)g^{\mu\nu}]\}.
\end{aligned} \tag{B48}$$

The values of A_{K_1}, B_{K_1}, and C_{K_1} depend on the process considered: $A_{K_1} = \{A_{K_1K^\star\pi}, A_{K_1\rho K}, A_{K_1\omega_N K}\}$ and $B_{K_1} = \{B_{K_1K^\star\pi}, B_{K_1\rho K}, B_{K_1\omega_N K}\}$. The coefficients read

$$A_{K_1K^\star\pi} = \frac{i}{\sqrt{2}}Z_\pi(h_3 - g_1^2)\phi_S, \tag{B49}$$

$$B_{K_1K^\star\pi} = -\frac{i}{2}Z_\pi g_2 w_{a_1}, \tag{B50}$$

$$\begin{aligned}
A_{K_1\rho K} = &\frac{i}{4}Z_K[g_1^2(\phi_N + \sqrt{2}\phi_S)\\
&- h_2(\phi_N - \sqrt{2}\phi_S) - 2h_3\phi_N],
\end{aligned} \tag{B51}$$

$$B_{K_1\rho K} = \frac{i}{2}Z_K g_2 w_{K_1}, \tag{B52}$$

$$\begin{aligned}
A_{K_1\omega_N K} = &-\frac{i}{4}Z_K[g_1^2(\phi_N + \sqrt{2}\phi_S)\\
&- h_2(\phi_N - \sqrt{2}\phi_S) - 2h_3\phi_N],
\end{aligned} \tag{B53}$$

$$B_{K_1\omega_N K} = -\frac{i}{2}Z_K g_2 w_{K_1}. \tag{B54}$$

[1] J. Beringer *et al.* (Particle Data Group), Phys. Rev. D **86**, 010001 (2012).

[2] C. Amsler and N. A. Tornqvist, Phys. Rep. **389**, 61 (2004); E. Klempt and A. Zaitsev, Phys. Rep. **454**, 1 (2007).

[3] A. V. Anisovich *et al.*, Phys. Lett. B **449**, 154 (1999); M. Ablikim *et al.* (BES Collaboration), Phys. Lett. B **603**, 138 (2004); **607**, 243 (2005); Phys. Rev. D **72**, 092002 (2005); D. V. Bugg, arXiv:hep-ph/0603018; A. V. Anisovich, D. V. Bugg, V. A. Nikonov, A. V. Sarantsev, and V. V. Sarantsev, Phys. Rev. D **85**, 014001 (2012).

[4] A. V. Anisovich and A. V. Sarantsev, Phys. Lett. B **413**, 137 (1997); R. Delbourgo and M. D. Scadron, Int. J. Mod. Phys. A **13**, 657 (1998); D. Black, A. H. Fariborz, S. Moussa, S. Nasri, and J. Schechter, Phys. Rev. D **64**, 014031 (2001); M. D. Scadron, F. Kleefeld, G. Rupp, and E. van Beveren, Nucl. Phys. **A724**, 391 (2003); D. V. Bugg, Phys. Lett. B **572**, 1 (2003); **595**, 556(E) (2004).

[5] S. N. Cherry and M. R. Pennington, Nucl. Phys. **A688**, 823 (2001); J. M. Link *et al.* (FOCUS Collaboration), Phys. Lett. B **621**, 72 (2005).

[6] I. Caprini, G. Colangelo, and H. Leutwyler, Phys. Rev. Lett. **96**, 132001 (2006); F. J. Yndurain, R. Garcia-Martin, and J. R. Pelaez, Phys. Rev. D **76**, 074034 (2007); H. Leutwyler, AIP Conf. Proc. **1030**, 46 (2008); R. Kaminski, R. Garcia-Martin, P. Grynkiewicz, and J. R.

Pelaez, Nucl. Phys. B, Proc. Suppl. **186**, 318 (2009); R. Garcia-Martin, R. Kaminski, J. R. Pelaez, and J. Ruiz de Elvira, Phys. Rev. Lett. **107**, 072001 (2011).
[7] D. V. Bugg, Eur. Phys. J. C **52**, 55 (2007).
[8] M. F. M. Lutz and E. E. Kolomeitsev, Nucl. Phys. **A730**, 392 (2004); M. Wagner and S. Leupold, Phys. Lett. B **670**, 22 (2008); Phys. Rev. D **78**, 053001 (2008); S. Leupold and M. Wagner, Int. J. Mod. Phys. A **24**, 229 (2009).
[9] A. Heinz, S. Struber, F. Giacosa, and D. H. Rischke, Phys. Rev. D **79**, 037502 (2009); Acta Phys. Polon. Supp. **3**, 925 (2010).
[10] S. Struber and D. H. Rischke, Phys. Rev. D **77**, 085004 (2008).
[11] C. Vafa and E. Witten, Nucl. Phys. **B234**, 173 (1984); L. Giusti and S. Necco, J. High Energy Phys. 04 (2007) 090.
[12] G. 't Hooft, Phys. Rep. **142**, 357 (1986).
[13] J. S. Schwinger, Ann. Phys. (N.Y.) **2**, 407 (1957); M. Gell-Mann and M. Levy, Nuovo Cimento **16**, 705 (1960); S. Weinberg, Phys. Rev. Lett. **18**, 188 (1967).
[14] J. S. Schwinger, Phys. Lett. **24B**, 473 (1967); S. Weinberg, Phys. Rev. **166**, 1568 (1968).
[15] D. Parganlija, F. Giacosa, and D. H. Rischke, Phys. Rev. D **82**, 054024 (2010).
[16] S. Gallas, F. Giacosa, and D. H. Rischke, Phys. Rev. D **82**, 014004 (2010).
[17] S. Gasiorowicz and D. A. Geffen, Rev. Mod. Phys. **41**, 531 (1969).
[18] P. Ko and S. Rudaz, Phys. Rev. D **50**, 6877 (1994).
[19] M. Urban, M. Buballa, and J. Wambach, Nucl. Phys. **A697**, 338 (2002).
[20] J. T. Lenaghan, D. H. Rischke, and J. Schaffner-Bielich, Phys. Rev. D **62**, 085008 (2000).
[21] P. Kovacs and Z. Szep, Phys. Rev. D **75**, 025015 (2007); **77**, 065016 (2008).
[22] J. Gasser and H. Leutwyler, Ann. Phys. (N.Y.) **158**, 142 (1984); see also S. Scherer, Adv. Nucl. Phys. **27**, 277 (2003) and references therein.
[23] M. Bando, T. Kugo, and K. Yamawaki, Phys. Rep. **164**, 217 (1988); G. Ecker, J. Gasser, A. Pich, and E. de Rafael, Nucl. Phys. **B321**, 311 (1989); E. E. Jenkins, A. V. Manohar, and M. B. Wise, Phys. Rev. Lett. **75**, 2272 (1995); C. Terschlusen and S. Leupold, Prog. Part. Nucl. Phys. **67**, 401 (2012).
[24] S. Janowski, D. Parganlija, F. Giacosa, and D. H. Rischke, Phys. Rev. D **84**, 054007 (2011).
[25] D. Parganlija, F. Giacosa, and D. H. Rischke, AIP Conf. Proc. **1030**, 160 (2008); Proc. Sci., CONFINEMENT 8 (2008) 070 [arXiv:0812.2183]; arXiv:0911.3996; Acta Phys. Polon. Supp. **3**, 963 (2010).
[26] D. Parganlija, F. Giacosa, D. H. Rischke, P. Kovacs, and G. Wolf, Int. J. Mod. Phys. A **26**, 607 (2011); D. Parganlija, F. Giacosa, P. Kovacs, and G. Wolf, AIP Conf. Proc. **1343**, 328 (2011); P. Kovacs, G. Wolf, F. Giacosa, and D. Parganlija, EPJ Web Conf. **13**, 02006 (2011); D. Parganlija, Acta Phys. Pol. B Proc. Suppl. **4**, 727 (2011); Phys. Scr. **T150**, 014029 (2012).
[27] C. Morningstar and M. J. Peardon, AIP Conf. Proc. **688**, 220 (2003); M. Loan, X. Q. Luo, and Z. H. Luo, Int. J. Mod. Phys. A **21**, 2905 (2006); E. B. Gregory, A. C. Irving, C. C. McNeile, S. Miller, and Z. Sroczynski, Proc. Sci., LAT2005 (2006) 027 [arXiv:hep-lat/0510066]; Y. Chen *et al.*, Phys. Rev. D **73**, 014516 (2006); C. M. Richards, A. Irving, E. Gregory, and C. McNeile (UKQCD Collaboration), Phys. Rev. D **82**, 034501 (2010).
[28] C. Amsler and F. E. Close, Phys. Rev. D **53**, 295 (1996); W. J. Lee and D. Weingarten, Phys. Rev. D **61**, 014015 (1999); F. E. Close and A. Kirk, Eur. Phys. J. C **21**, 531 (2001); F. Giacosa, T. Gutsche, V. E. Lyubovitskij, and A. Faessler, Phys. Rev. D **72**, 094006 (2005); Phys. Lett. B **622**, 277 (2005); F. Giacosa, T. Gutsche, and A. Faessler, Phys. Rev. C **71**, 025202 (2005); H. Y. Cheng, C. K. Chua, and K. F. Liu, Phys. Rev. D **74**, 094005 (2006); L. Bonanno and A. Drago, Phys. Rev. C **79**, 045801 (2009); V. Mathieu, N. Kochelev, and V. Vento, Int. J. Mod. Phys. E **18**, 1 (2009).
[29] D. Parganlija, Ph.D. thesis, Institute for Theoretical Physics of Frankfurt University, 2012.
[30] U. G. Meissner, Phys. Rep. **161**, 213 (1988).
[31] F. Giacosa, Phys. Rev. D **80**, 074028 (2009).
[32] C. Rosenzweig, A. Salomone, and J. Schechter, Phys. Rev. D **24**, 2545 (1981); A. Salomone, J. Schechter, and T. Tudron, Phys. Rev. D **23**, 1143 (1981); C. Rosenzweig, A. Salomone, and J. Schechter, Nucl. Phys. **B206**, 12 (1982); **B207**, 546(E) (1982); A. A. Migdal and M. A. Shifman, Phys. Lett. **114B**, 445 (1982); H. Gomm and J. Schechter, Phys. Lett. **158B**, 449 (1985); R. Gomm, P. Jain, R. Johnson, and J. Schechter, Phys. Rev. D **33**, 801 (1986).
[33] E. Witten, Nucl. Phys. **B160**, 57 (1979); S. R. Coleman, in *Pointlike Structures Inside and Outside Hadrons*, edited by A. Zichichi (Plenum Press, New York, 1982), p. 0011; R. F. Lebed, Czech. J. Phys. **49**, 1273 (1999).
[34] D. M. Asner *et al.* (CLEO Collaboration), Phys. Rev. D **61**, 012002 (1999).
[35] C. Bromberg, J. Dickey, G. Fox, R. Gomez, W. Kropac, J. Pine, S. Stampke, H. Haggerty *et al.*, Phys. Rev. D **22**, 1513 (1980).
[36] C. Dionisi *et al.* (CERN-College de France-Madrid-Stockholm Collaboration), Nucl. Phys. **B169**, 1 (1980).
[37] F. Giacosa and G. Pagliara, Nucl. Phys. **A833**, 138 (2010).
[38] M. Harada and K. Yamawaki, Phys. Rep. **381**, 1 (2003).
[39] L. Burakovsky and J. T. Goldman, Phys. Rev. D **57**, 2879 (1998).
[40] A. A. Osipov, B. Hiller, A. H. Blin, and J. da Providencia, Ann. Phys. (Amsterdam) **322**, 2021 (2007).
[41] D. Black, A. H. Fariborz, and J. Schechter, Phys. Rev. D **61**, 074001 (2000).
[42] D. Black, A. H. Fariborz, F. Sannino, and J. Schechter, Phys. Rev. D **59**, 074026 (1999); A. H. Fariborz, R. Jora, and J. Schechter, Phys. Rev. D **72**, 034001 (2005); **76**, 014011 (2007); **77**, 034006 (2008); **79**, 074014 (2009); A. H. Fariborz, R. Jora, J. Schechter, and M. N. Shahid, Phys. Rev. D **83**, 034018 (2011); **84**, 113004 (2011); T. K. Mukherjee, M. Huang, and Q.-S. Yan, arXiv:1203.5717.
[43] F. Giacosa, Phys. Rev. D **75**, 054007 (2007).
[44] F. Giacosa and T. Wolkanowski, arXiv:1209.2332.
[45] F. Giacosa and G. Pagliara, Phys. Rev. C **76**, 065204 (2007).
[46] J. R. Pelaez, Mod. Phys. Lett. A **19**, 2879 (2004).
[47] E. van Beveren, T. A. Rijken, K. Metzger, C. Dullemond, G. Rupp, and J. E. Ribeiro, Z. Phys. C **30**, 615 (1986); N. A. Tornqvist, Z. Phys. C **68**, 647 (1995); M. Boglione

and M. R. Pennington, Phys. Rev. D 65, 114010 (2002); E. van Beveren, D. V. Bugg, F. Kleefeld, and G. Rupp, Phys. Lett. B **641**, 265 (2006); J. A. Oller, E. Oset, and J. R. Pelaez, Phys. Rev. D **59**, 074001 (1999); **60**, 099906(E) (1999).

[48] V. A. Polychronakos, N. Cason, J. Bishop, N. Biswas, V. Kenney, D. Rhines, R. Ruchti, W. Shephard, M. Stangl, and J. Watson, Phys. Rev. D **19**, 1317 (1979); A. B. Wicklund, D. S. Ayres, D. H. Cohen, R. Diebold, and A. J. Pawlicki, Phys. Rev. Lett. **45**, 1469 (1980); A. Etkin *et al.*, Phys. Rev. D **25**, 1786 (1982); B. V. Bolonkin *et al.*, Yad. Fiz. **46**, 799 (1987) [Nucl. Phys. **B309**, 426 (1988)]; G. D. Tikhomirov, I. A. Erofeev, O. N. Erofeeva, and V. N. Luzin, Phys. At. Nucl. **66**, 828 (2003) [Yad. Fiz. **66**, 860 (2003)]; V. V. Vladimirsky *et al.*, Phys. At. Nucl. **69**, 493 (2006) [Yad. Fiz. **69**, 515 (2006)].

[49] M. Ablikim *et al.* (BES Collaboration), Phys. Lett. B **607**, 243 (2005).

[50] M. Bargiotti *et al.* (OBELIX Collaboration), Eur. Phys. J. C **26**, 371 (2003).

[51] D. Barberis *et al.* (WA102 Collaboration), Phys. Lett. B **462**, 462 (1999).

[52] M. Ablikim *et al.*, Phys. Lett. B **642**, 441 (2006).

[53] D. Barberis *et al.* (WA102 Collaboration), Phys. Lett. B **479**, 59 (2000).

[54] V. V. Anisovich, V. A. Nikonov, and A. V. Sarantsev, Phys. At. Nucl. **65**, 1545 (2002) [Yad. Fiz. **65**, 1583 (2002)].

[55] M. S. Bhagwat, L. Chang, Y.-X. Liu, C. D. Roberts, and P. C. Tandy, Phys. Rev. C **76**, 045203 (2007); F. Ambrosino, A. Antonelli, M. Antonelli, F. Archilli, P. Beltrame, G. Bencivenni, S. Bertolucci, C. Bini *et al.*, J. High Energy Phys. 07 (2009) 105; G. Amelino-Camelia, F. Archilli, D. Babusci, D. Badoni, G. Bencivenni, J. Bernabeu, R. A. Bertlmann, D. R. Boito *et al.*, Eur. Phys. J. C **68**, 619 (2010); M. C. Chang, Y. C. Duh, J. Y. Lin, I. Adachi, K. Adamczyk, H. Aihara, D. M. Asner, T. Aushev *et al.*, Phys. Rev. D **85**, 091102 (2012).

[56] R. K. Carnegie, R. J. Cashmore, W. M. Dunwoodie, T. A. Lasinski, and D. W. G. Leith, Phys. Lett. **68B**, 287 (1977); J. L. Rosner, Comments Nucl. Part. Phys. **16**, 109 (1986); N. Isgur and M. B. Wise, Phys. Lett. B **232**, 113 (1989); H. G. Blundell, S. Godfrey, and B. Phelps, Phys. Rev. D **53**, 3712 (1996); F. E. Close and A. Kirk, Z. Phys. C **76**, 469 (1997); D. M. Li, H. Yu, and Q. X. Shen, Chin. Phys. Lett. **17**, 558 (2000); D. M. Asner *et al.* (CLEO Collaboration), Phys. Rev. D **62**, 072006 (2000); W. S. Carvalho, A. S. de Castro, and A. C. B. Antunes, J. Phys. A **35**, 7585 (2002); H. Y. Cheng, Phys. Rev. D **67**, 094007 (2003); T. Barnes, N. Black, and P. R. Page, Phys. Rev. D **68**, 054014 (2003); D. M. B. Li, B. Ma, Y. X. Li, Q. K. Yao, and H. Yu, Eur. Phys. J. C **37**, 323 (2004); J. Vijande, F. Fernandez, and A. Valcarce, J. Phys. G **31**, 481 (2005); D. M. Li, B. Ma, and H. Yu, Eur. Phys. J. A **26**, 141 (2005); D. M. Li and Z. Li, Eur. Phys. J. A **28**, 369 (2006); H. Hatanaka and K. C. Yang, Phys. Rev. D **77**, 094023 (2008); **78**, 059902(E) (2008); H. Y. Cheng and C. K. Chua, Phys. Rev. D **81**, 114006 (2010); **82**, 059904(E) (2010); K.-C. Yang, Phys. Rev. D **84**, 034035 (2011); H.-Y. Cheng, Phys. Lett. B **707**, 116 (2012).

[57] T. Hatsuda and S. H. Lee, Phys. Rev. C **46**, R34 (1992).

[58] G. Brown and M. Rho, Phys. Rev. Lett. **66**, 2720 (1991).

[59] P. Salabura, Acta Phys. Pol. B **27**, 421 (1996); G. Agakichiev *et al.*, Phys. Lett. B **422**, 405 (1998).

[60] R. L. Jaffe, Phys. Rev. D **15**, 267 (1977); **15**, 281 (1977); L. Maiani, F. Piccinini, A. D. Polosa, and V. Riquer, Phys. Rev. Lett. **93**, 212002 (2004); M. Napsuciale and S. Rodriguez, Phys. Rev. D **70**, 094043 (2004); F. Giacosa, Phys. Rev. D **74**, 014028 (2006).

[61] W. Heupel, G. Eichmann, and C. S. Fischer, Phys. Lett. B **718**, 545 (2012).

[62] C. Michael, A. Shindler, and M. Wagner (ETM Collaboration), J. High Energy Phys. 08 (2010) 009; R. Baron, P. Boucaud, J. Carbonell, A. Deuzeman, V. Drach, F. Farchioni, V. Gimenez, G. Herdoiza *et al.*, J. High Energy Phys. 06 (2010) 111; R. Baron *et al.* (European Twisted Mass Collaboration), Comput. Phys. Commun. **182**, 299 (2011); M. Wagner (ETM and Y Collaborations), Proc. Sci., LATTICE 2010 (2010) 162 [arXiv:1008.1538]; R. Baron *et al.* (ETM Collaboration), arXiv:1009.2074; Proc. Sci., LATTICE 2010 (2010) 123 [arXiv:1101.0518]; M. Wagner (ETM Collaboration), Acta Phys. Pol. B Proc. Suppl. **4**, 747 (2011).

[63] T. Sakai and S. Sugimoto, Prog. Theor. Phys. **113**, 843 (2005); **114**, 1083 (2005); D. Li, M. Huang, and Q.-S. Yan, arXiv:1206.2824.

[64] S. Gallas, F. Giacosa, and G. Pagliara, Nucl. Phys. **A872**, 13 (2011).

[65] A. Schmitt, S. Stetina, and M. Tachibana, Phys. Rev. D **83**, 045008 (2011); F. Preis, A. Rebhan, and A. Schmitt, J. High Energy Phys. 03 (2011) 033; J. Phys. G **39**, 054006 (2012).